



**HAL**  
open science

## Multifactorial effects of warming, low irradiance, and low salinity on Arctic kelps

Anaïs Lebrun, Cale Andrew Miller, Marc Meynadier, Steeve Comeau, Pierre Urrutti, Samir Alliouane, Robert Schlegel, Jean-Pierre Gattuso, Frédéric Gazeau

► **To cite this version:**

Anaïs Lebrun, Cale Andrew Miller, Marc Meynadier, Steeve Comeau, Pierre Urrutti, et al.. Multifactorial effects of warming, low irradiance, and low salinity on Arctic kelps. 2023. hal-04236891

**HAL Id: hal-04236891**

**<https://hal.science/hal-04236891>**

Preprint submitted on 11 Oct 2023

**HAL** is a multi-disciplinary open access archive for the deposit and dissemination of scientific research documents, whether they are published or not. The documents may come from teaching and research institutions in France or abroad, or from public or private research centers.

L'archive ouverte pluridisciplinaire **HAL**, est destinée au dépôt et à la diffusion de documents scientifiques de niveau recherche, publiés ou non, émanant des établissements d'enseignement et de recherche français ou étrangers, des laboratoires publics ou privés.



## Multifactorial effects of warming, low irradiance, and low salinity on Arctic kelps

Anaïs Lebrun<sup>1</sup>, Cale A. Miller<sup>1,2</sup>, Marc Meynadier<sup>3</sup>, Steeve Comeau<sup>1</sup>, Pierre Urrutti<sup>1</sup>, Samir Alliouane<sup>1</sup>, Robert Schlegel<sup>1</sup>, Jean-Pierre Gattuso<sup>1,4</sup>, Frédéric Gazeau<sup>1</sup>

<sup>1</sup> Laboratoire d'Océanographie de Villefranche, Sorbonne Université, CNRS, Villefranche-sur-Mer, France

<sup>2</sup> Department of Earth Sciences, Utrecht University, Utrecht, The Netherlands

<sup>3</sup> Laboratoire de Biologie du Développement de Villefranche-sur-mer, Sorbonne Université, CNRS, Villefranche-sur-Mer, France

<sup>4</sup> Institute for Sustainable Development and International Relations, Sciences Po, Paris, France

Correspondence to: Anaïs Lebrun (anaïs.lebrun@imev-mer.fr)

10

Abstract

The Arctic is projected to warm by 2 to 5°C by the end of the century. Warming causes melting of glaciers, shrinking of the areas covered by sea ice, and increased terrestrial runoff from snowfields and permafrost thawing. Warming, decreasing coastal underwater irradiance, and lower salinity are potentially threatening polar marine organisms, including kelps, that are key species of hard-bottom shallow communities. The present study investigates the physiological responses of four kelp species (*Alaria esculenta*, *Laminaria digitata*, *Saccharina latissima*, and *Hedophyllum nigripes*) to warming, low irradiance, and low salinity through a perturbation experiment conducted in *ex situ* mesocosms. Kelps were exposed during six weeks to four experimental treatments: an unmanipulated control, a warming condition mimicking future coastlines unimpacted by glacier melting under the CO<sub>2</sub> emission scenario SSP5-8.5, and two multifactorial conditions combining warming, low salinity, and low irradiance reproducing the future coastal Arctic exposed to terrestrial runoff following two CO<sub>2</sub> emission scenarios (SSP2-4.5 and SSP5-8.5). The physiological effects on *A. esculenta*, *L. digitata* and *S. latissima* were investigated and gene expression patterns of *S. latissima* and *H. nigripes* were analyzed. Specimens of *A. esculenta* increased their chlorophyll *a* content when exposed to low irradiance conditions, suggesting that they may be resilient to an increase in glacier and river runoff and become more dominant at greater depths. *S. latissima* showed a lower carbon:nitrogen (C:N) ratio at higher nitrate concentrations, suggesting coastal erosion and permafrost thawing could benefit the organism in the future Arctic. In contrast, *L. digitata* showed no responses to the conditions tested on any of the investigated physiological parameters. The gene expressions of *H. nigripes* and *S. latissima* underscores their ability and underline temperature as a key influencing factor. Based on these results, it is expected that kelp communities will undergo changes in species composition that will vary at local scale as a function of the changes in environmental drivers. For future research, potential cascading effects on the associated fauna and the whole ecosystem are important to anticipate the ecological, cultural, and economic impacts of climate change in the Arctic.



## 35 1. Introduction

The Arctic region is warming at more than twice the global average rate (Richter-Menge et al., 2017). Over the next 80 years, sea surface temperature is projected to increase by 2 °C according to the Shared Socio-economic Pathways (SSP) 1-2.6, which foresees an increasing shift towards sustainable practices, and up to 5°C according to the SSP5-8.5, which assumes an energy-intensive and fossil fuel-based economy  
40 (Kwiatkowski et al., 2020). Warming induces glacier and sea ice to melt at a faster rate causing an increase in terrestrial runoff from thawing snowfields and permafrost (Shiklomanov and Shiklomanov 2003; Stroeve et al., 2014). Total freshwater inflow into the Arctic Ocean rose by around 7% between 1936 and 1999 and 14% between 1980 and 2009 (Peterson et al., 2002; Ahmed et al., 2020). Combined with vertical mixing by waves and wind action, cryosphere melting results in local turbid and low-salinity waters down to 20 m (Karsten  
45 2007). Coastal areas are therefore exposed to warming, changing light and salinity conditions (Lebrun et al., 2022).

In the coastal Arctic, kelps are key ecosystem engineers. Kelp forests provide a food source, habitat, and nursery ground for numerous fish and invertebrates as well as protect the coast from erosion (Filbee-Dexter et al., 2019). They support complex food webs and have a substantial role in storing and sequestering carbon  
50 (Krause-Jensen and Duarte 2016). *Saccharina latissima*, *Alaria esculenta*, *Laminaria digitata*, and *Hedophyllum nigripes* are four abundant kelp species that inhabit the northern hemisphere and extend to subarctic and Arctic waters (Bischof et al., 1999; Müller et al. 2009). As a result of warming, which induces more sea ice-free areas, the surface area suitable for kelps has increased by about 45% from 1940-1950 to 2000-2017 (Krause-Jensen et al., 2020). Temperature requirements and seasonal variability tolerance in  
55 irradiance and salinity for reproduction and growth determine the geographical distribution of kelp species (Wiencke et al. 1994, Muth et al., 2021). Irradiance has a major impact on their depth distribution (e.g. Roleda et al. 2005; Krause-Jensen et al., 2012). Turbid waters alter kelp fitness by limiting photosynthesis. This has already induced a shift in the vertical distribution of kelps such as *Laminaria* and *Saccharina* genera to shallower waters (Bartsch et al., 2016; Filbee-Dexter et al., 2019). Because optimal temperature, irradiance,  
60 and salinity ranges vary between kelp species, their response to environmental changes will likely be species-specific (Eggert 2012; Karsten 2012).

We hypothesized that (1) warming will enhance the growth rate of kelps during summer, and (2) that the combined effects of high temperature, low salinity and low irradiance will negatively impact their physiology, although responses will be species-specific. To test these hypotheses and fill knowledge gaps on the  
65 multifactorial effects of climate change across species (Renaud et al., 2019; Scherrer et al., 2019), we carried out a land-based mesocosm experiment exposing four kelp species (*S. latissima*, *A. esculenta*, *L. digitata*, and *H. nigripes*) to four treatments for six weeks. The treatments consisted of a control, a warming condition mimicking the future offshore (T1), and two multifactorial conditions combining warming, low salinity, and low irradiance mimicking the future coastal Arctic (T2 and T3). In order to best represent *in situ* conditions,  
70 the different kelp species were incubated together in each mesocosm at densities mimicking natural



communities. The physiological effects on *A. esculenta*, *L. digitata* and *S. latissima* were investigated and gene expression patterns of *S. latissima* and *H. nigripes* were analyzed.

## 2. Material and methods

### 75 2.1 Specimen collection

In June 2021, 188 sporophytes of *A. esculenta*, *L. digitata*, *S. latissima*, and *H. nigripes* shorter than 1 m were collected by research divers in Kongsfjorden (Svalbard, Norway). They were collected between 2 and 7 m depth at Hansneset and the Old Pier (Fig. 1). All samples were placed into holding tanks ( $> 1 \text{ m}^3$ ) until their placement into final mesocosms on 2021-07-03.

80

### 2.2 Mesocosm experiment

The experiment was carried out from 2021-07-03 ( $t_0$ ) to 2021-08-28 ( $t_{\text{final}}$ ), in twelve  $1 \text{ m}^3$  mesocosms set up in Ny-Ålesund on the outdoor platform of the Kings Bay Marine Laboratory in order to expose communities to natural light cycles. Each mesocosm received 3 to 6 individuals of *A. esculenta* and *S. latissima*, 2 to 4  
85 individuals of *L. digitata* and 0 to 2 individuals of *H. nigripes* for a total mass (wet weight) of kelp biomass per mesocosm of about 1500 g for *S. latissima* and *L. digitata* (mingled with *H. nigripes*) and 1000 g for *A. esculenta*. These biomasses are representative of those found at Hansneset down to 7 m depth (Hop et al., 2012). Since *H. nigripes* can be mistaken for *L. digitata*, each stipe of these two species was cut at  $t_{\text{final}}$  to detect individuals with mucilage, corresponding to *H. nigripes* ( $n=16$ , Dankworth et al., 2020).

90 The experimental set-up is briefly described below. More information can be found in Miller et al. (under revision). Seawater flowing through the mesocosms was pumped from 10 m depth in front of the Kings Bay Marine Laboratory (78.929°N, 11.930°E) using a submersible pump (Albatros©). The regulated flow-through system ( $7 - 8 \text{ L min}^{-1}$  in each mesocosm) allowed for the automated control of temperature and salinity. Temperature was adjusted by mixing ambient seawater with warmed seawater ( $15^\circ\text{C}$ ) and salinity was  
95 regulated by addition of freshwater. Each mesocosm was equipped with one 12 W wave pump (Sunsun© JVP-132) to ensure proper mixing.

Four experimental treatments in triplicate (4x3 mesocosms) were used to study conditions representative of present and future Arctic coastal communities at proximity or not to glaciers following two different SSP scenarios (Ctrl, T1, T2, T3; Table 1). Treatments 1 and 2 (T1 and T2) mimicked the conditions expected close  
100 to glaciers and, therefore, combined warming, low irradiance, and low salinity. T1 followed the SSP 2-4.5, which describes a middle-of-the-road projection that does not shift markedly from historical patterns, while T2 followed the SSP5-8.5 that assumes an energy-intensive and fossil fuel-based economy. T3 focused on the projected change outside glacials fjords following the SSP 5-8.5, where warming acts as a single driver. Temperature was increased by  $3.3^\circ\text{C}$  in T1 and  $5.3^\circ\text{C}$  in T2 and T3 as an offset increase from the control  
105 condition (Ctrl) which mimicked the *in situ* temperature recorded in real-time during the whole experiment. Based on *in situ* measurements taken from week 22 to 35 in 2020 in the Kongsfjorden, salinity offsets were



determined from the *in situ* relationship between temperature and salinity and extrapolated to apply to future warming. This resulted in a salinity decreased by 2.5 in T1 and 5 in T2 (Miller et al., under revision). Based on *in situ* photosynthetically active radiation (PAR) data collected in May 2021 with a LICOR, irradiance was  
110 reduced from the control by a mean of 20% for T1, corresponding to the difference between the glacier-proximal inner region and the middle of the fjord, and 30% for T2, corresponding to the difference the inner and outer parts of the fjord. To simulate the *in situ* light spectrum (Kai Bischof, pers. com.) and reach the irradiance matching the targeted treatments, green (RL244) and neutral Lee filters<sup>©</sup> (RL211; RL298) were placed on top of mesocosms (Table 1). During the first week, all the mesocosms were maintained under *in situ*  
115 conditions of temperature, salinity, and irradiance. The light filters were then added to the mesocosms of T1 and T2 treatments on 2021-07-10 and all treatments gradually reached their targeted temperature and salinity conditions in six days. The experiment then lasted for six weeks.

### 2.3 Tissue sampling

120 Tissue samples were collected in the meristem of ten individuals of *A. esculenta*, *L. digitata*, and *S. latissima* at the beginning of the experiment ( $t_0$ , 2021-07-03) and on the healthy organisms, namely complete organisms (frond, stipe, and holdfast) that exhibit a firm brown frond without signs of disease at the end ( $t_{\text{final}}$ ) pending determination of chlorophyll *a* (chl *a*, see section 2.3) and carbon:nitrogen (C:N) ratio (see section 2.4). Samples were stored in aluminum foil at -20°C. Additional tissue samples were collected in the meristem of  
125 *S. latissima* and *H. nigripes* at  $t_{\text{final}}$  for gene expression analysis (n=8 for each species, see section 2.7) and immediately flash-frozen in liquid nitrogen before being stored at -80°C.

### 2.4 Chl *a* content

Samples were blotted dry, weighed (wet weight), and ground with a glass pestle. Chl *a* was extracted in 90%  
130 aqueous acetone for 24 h in the dark at 4°C. After cold-centrifugation (0°C, 15 min, 3000 rpm), the supernatants were transferred one at a time into a glass vial and the initial fluorescence ( $F_0$ ) of chl *a* and pheophytin pigment were measured using a fluorimeter (Turner Design 10-AU Fluorimeter; 667 nm). The  $F_a$  fluorescence was measured one minute after the addition of 10  $\mu\text{l}$  of 0.3 N HCl to transform chl *a* into pheophytin pigment and subtract  $F_a$  from  $F_0$ . The chl *a* content was calculated using the formula of Lorenzen  
135 (1967). Chl *a* content are expressed in  $\mu\text{g}$  per g of fresh weight ( $\mu\text{g gFW}^{-1}$ ).

### 2.5 C:N ratio

Samples were dried at 60°C for 48 h, weighed (dry weight), and their sizes adjusted to ensure that they did not weigh more than 10 mg, the detection limits specific to the CHN analyzer (PerkinElmer, Inc 2400). C and N  
140 contents are expressed in  $\mu\text{g}$  per g of dry weight ( $\mu\text{g gDW}^{-1}$ ).



## 2.6 Growth rate

Growth rate was determined using the hole puncture method of Parke (1948). Sporophytes were punctured at  $t_0$  in the meristem section of each organism, 2 cm from the base of the stipe. The distance from the base of the 145 stipe to the hole was measured at  $t_{final}$ . The growth rate was calculated as follows:

$$Growth\ rate\ (cm.\ d^{-1}) = \frac{dist_{final} - dist_0}{t_{final} - t_0}$$

with dist: distance (in cm) from the base of the stipe to the meristem at time t (in days)

150 Weekly growth rates for selected individuals was also determined at different time points during the experiment for *S. latissima* (weeks 1 and 4) and *A. esculenta* (weeks 2 and 5). Results can be found in the supplementary material (Fig. A1).

## 2.7 Gene expression analysis

155 Total RNA extraction was conducted using the method described by Heinrich et al. (2012). The quantity and purity of the extracted RNA were evaluated using a Nanodrop ND-1000 Spectrophotometer (ThermoFisher), which measures RNA concentration at 260 nm and assesses purity by detecting the presence of other compounds such as DNA at 230 nm and proteins at 280 nm. The integrity of total RNA was determined by automated capillary electrophoresis using an Agilent 2100 Bioanalyzer (Agilent Technologies). The cDNA 160 libraries were constructed by poly(A) enrichment and sequenced on a NovaSeq 6000 instrument by the Genome Quebec platform. The 100 bp paired reads were clipped using default values of the Illumina software. The quality of raw sequences was checked using FastQC v.0.11.7 (<https://www.bioinformatics.babraham.ac.uk/projects/fastqc/>). Sequences of low quality were trimmed using Trimmomatic v.0.39 (Bolger et al., 2014). For each species, a *de novo* transcriptome was constructed using 165 the Trinity v.2.14.0 tool (Grabherr et al., 2011). The most homologous sequences were clustered using the CD-HIT-EST algorithm, part of the CD-HIT v.4.8.1 tool (Li and Godzik, 2006). To ensure the quality of the *de novo* transcriptomes, another transcriptome per species was generated using the maSPAdes v.3.14.1 (Bushmanova et al., 2019). Transcriptomes generated with maSPAdes and Trinity were compared using BUSCO v.5.4.3, transcriptomes generated with Trinity were retained due to lower duplicated sequences 170 (Simão et al., 2015). Transcript quantification was performed by pseudo alignment using Kallisto v0.46.0, mapping RNA sequences to an index created from *de novo* transcriptomes (Bray et al., 2016). Exploration of differentially expressed genes (DEGs) was performed with the DESeq2 v1.34.0 R package (Love et al., 2014). For each species, DEGs were obtained from the following comparisons: T1 vs. C, T2 vs. C, T3 vs. C, T2 vs. T1, T3 vs. T1, and T3 vs. T2. Transcripts with an adjusted  $p < 0.05$  and  $\log_2$  fold change (FC)  $> 2$  or  $< -2$  were 175 considered significantly differentially expressed genes. Functional annotation of the genes was performed with eggNOG-mapper v2.1.10 against the eggNOG database v.5.0.2 (Huerta-Cepas et al., 2017 & 2019). To ensure



they were properly annotated, annotation was also performed with TransDecoder v5.5.0 to predict coding sequences (Haas and Papanicoualo, 2015), which were aligned against a Pfam profile database v35.0 (Mistry et al., 2021) using the HMMER v3.3 alignment tool (Finn et al., 2011). Gene Ontology (Gene Ontology Consortium, 2015) terms were then retrieved from the pfam2go database (<https://pypi.org/project/pfam2go/>) and functional enrichment was performed with Ontologizer v2.1 to obtain statistically significant GOs from the DEGs of each comparison performed previously (Bauer et al., 2008). Functional enrichment results were summarized as tree plots and scatter plots using REVIGO v1.8.1 (Supek et al., 2011). Investigation of the specific functions of DEGs was carried out by manually checking the involvement of Pfam domains and EggNOG annotations on the SMART database v9.0 (Letunic et al., 2021). Some DEGs whose annotation was questionable (i.e. not referring to plant genomes such as gene collagen) were removed, as well as those whose annotation was not precise enough to be classified. DEGs were then classified into different categories: cytoskeleton, genetic transcription/translation, metabolism, signaling, transport, stress (heat stress and oxydo-reduction processes), and energy production (respiration and photorespiration). A part of DEGs (73.2% in *S. latissima* and 82.3% in *H. nigripes*) were trimmed as they lacked functional annotation. Tools and parameters are summarized in Table S1.

## 2.8 Statistics

Rosner's generalized Extreme Studentized Deviation (ESD) test was used to detect the outliers using the function `rosnerTest` of the R package `EnvStats` (Millard, 2013). Out of a total of 165 individual chl *a* measurements, when combining all species and conditions, eleven were identified as outliers and removed. After the removal of the outliers, the normal distribution of the data was verified with a Shapiro-Wilk test using the function `shapiro.test` from the stats R package (R Core Team, 2013) ( $p > 0.105$ ). No outliers were identified in the C:N and growth rate data and normality was verified ( $p > 0.089$ ).

Chl *a* content and C:N were analyzed using a linear mixed model with a hierarchical structure (HLM) to evaluate treatment effects by species. The model was fitted using the function `lmer` in the R package `lme4` (Bates et al., 2015). The fixed factors for the model were treatment and species, while mesocosm was a random factor. For growth rate measurements, a generalized linear mixed model (GLMM) with a Gaussian distribution was preferred - based on an Akaike information criterion - to test for the effects of the species, treatment, and mesocosm replica.

## 3. Results

### 3.1 Experimental conditions

The median temperature value in the control treatment was 5.3°C during the experimental period (2021-07-16 to 2021-08-28) calculated based on the mean value across replicates (Fig. 2, Table 1). The median salinity was 33.8 and the median daily PAR was 47.8  $\mu\text{mol photons m}^{-2} \text{s}^{-1}$ . In treatment T1, the median temperature, salinity, and PAR were 8.9°C, 31, and 36.1  $\mu\text{mol photons m}^{-2} \text{s}^{-1}$ , respectively. For treatments T2 and T3, the



median temperature was elevated to 10.8°C. In T2, median salinity and PAR were decreased to 28.5, and 31.4  $\mu\text{mol photons m}^{-2} \text{ s}^{-1}$ .

### 215 3.2 Chl *a* content

For *A. esculenta*, the concentration of chl *a* decreased significantly between  $t_0$  and the control at  $t_{\text{final}}$  ( $p < 0.01$ , Fig. 3, Tables D1, D2). Values in the T2 treatment were also significantly different from the control, T1, and T3 treatments (all  $p$  were  $< 0.01$ ). Values in the control, T1, and T3 treatments were not statistically different from each other ( $p > 0.92$ ).

220 Similarly to *A. esculenta*, chl *a* content of *S. latissima* significantly decreased between  $t_0$  and  $t_{\text{final}}$  ( $p = 0.02$ ) for the control, but were not significantly impacted by the treatments ( $p > 0.99$ ).

The chl *a* content of *L. digitata* was not significantly impacted by time and treatments ( $p > 0.99$ ).

### 3.3 C:N ratio

225 For *S. latissima*, C:N ratios at  $t_0$  ranged from 24.5 up to 37.1 (Fig. 4). No statistical difference was found between  $t_0$ , the control, T1, and T3 treatment at  $t_{\text{final}}$  ( $p > 0.93$ , Tables E1, E2). In contrast, C:N ratios of individuals in the T2 treatment were significantly lower than at  $t_0$ , ranging from 15.2 to 29.5 (Fig. 4A,  $p = 0.045$ ). Although carbon content showed no significant difference across treatments and time (Fig. 4B,  $p = 1$ ), there was a notable increase in nitrogen content in the T2 treatment compared to  $t_0$ , but it was not statistically significant (Fig. 4C,  $p = 0.06$ ).

230 The C:N ratios, carbon, and nitrogen contents of *A. esculenta* and *L. digitata* were not significantly impacted by the treatments ( $p > 0.32$ ).

### 3.4 Growth rate

235 The growth rates of *A. esculenta*, *L. digitata*, and *S. latissima* were not significantly impacted by the treatments (Fig. 5,  $p = 1$ , Tables F1, F2). They ranged from 0 to 0.037  $\text{cm d}^{-1}$  for *A. esculenta*, 0.007 to 0.046  $\text{cm d}^{-1}$  for *L. digitata*, and 0.040 up to 0.509  $\text{cm d}^{-1}$  for *S. latissima*. The growth rate of *S. latissima* was significantly higher than for the two other species for each treatment ( $p < 0.01$ ).

240 The growth rate of *A. esculenta* significantly decreased between week 2 and week 6 ( $p < 0.01$ , Fig. A1-A) over time in the control. For *S. latissima*, no significant differences were found over time in the C, T1 and T2, except in the T3 treatment ( $p=0.02$ , Fig. A1-B). No intermediate measurements of *L. digitata* growth rate were taken.

### 3.5 Gene expression analysis

245 The analysis of gene expression revealed a clear contrast between the control and the different treatments for both *S. latissima* and *H. nigripes* (Fig. B1). The number of total differentially expressed genes (DEGs, i.e. genes that are either up- or down-regulated when comparing the different treatments to the control) were close between *S. latissima* (831 including 225 classified) and *H. nigripes* (815 including 144 classified, Fig. 6A) and





mostly down-regulated for both species (84 and 65% respectively). For *H. nigripes*, the majority of overlapping  
250 DEGs were found between treatments T1 and T2 (Fig. 6A). Conversely, for *S. latissima*, the highest number  
of overlapping DEGs was observed between treatments T1 and T3. In both species, no overlapping genes were  
identified when comparing the DEGs between treatment pairs T1 vs. T2 and T2 vs. T3 (Fig. 6B).

The highest number of DEGs were exhibited in the transcription/translation and metabolism classes in *H.*  
*nigripes* (Fig. 7A) and in the transcription/translation and cytoskeleton classes for *S. latissima* (Fig. 7B). For  
255 this last species, the T3 treatments caused the highest number of down-regulated genes (607 including 152  
classified) with 60% belonging to the three classes mentioned above, followed by T1 (314 including 47  
classified) and T2 (247 including 56 classified; Fig. 6 and 7). For *H. nigripes*, 600 genes were observed to be  
regulated in T2 including 458 genes down-regulating. A substantial portion of the classified down-regulating  
genes belongs to the transcription/translation and metabolism class (64%), followed by an approximately equal  
260 proportion of genes associated with photorespiration (13%), stress (11%), and transport (8%) and lesser  
proportions of genes associated with other functions.

Genes belonging to the photorespiration/energy production class, involved either in the photosynthesis or  
respiration process, were found to be down-regulated in *H. nigripes* in T2 and in *S. latissima* in T2 and T3.  
Stress genes were down-regulated in all treatments for both species.

265

#### 4. Discussion

The analysis of gene expression combined with the investigated physiological parameters show the ability of  
Arctic kelps to acclimate to a range of environmental conditions. Indeed, no negatively impacts of the  
treatments was recorded, even according to the highest emissions scenario (SSP5-8.5). This observation  
270 confirms that these species, originating from lower latitudes, could thrive in a warmer Arctic. This also refutes  
our hypothesis that the combined effects of high temperature, low salinity, and low irradiance will necessarily  
have a negative impact on their physiology.

##### 4.1 Chl *a* content

275 We hypothesized that different species might have different responses to a changing environment. The chl *a*  
content of both *A. esculenta* and *S. latissima* in the meristem part of the frond showed a significant decrease  
from  $t_0$  to  $t_{final}$  in the control (-45% and -70% respectively). The same trend was observed in *L. digitata* although  
this is not significant due to the low number of measurements (-57%,  $n=3$  at  $t_{final}$ ). The high level of chl *a*  
measured in early summer matches the anticipation of ice melting and the following increase in turbidity  
280 (Aguilera et al., 2002). Decreasing chl *a* content between June and August has already been reported *in situ*  
in Kongsfjorden for *S. latissima* (Aguilera et al., 2002) with the end of the growth period (Berge et al., 2020).

In contrast to what was observed in the control as well as in the T1 and T3 treatments, for *A. esculenta*, the chl  
*a* content in the warm, less saline, and with lower irradiance treatment (T2) remained as high as it was at  $t_0$ .  
The decrease in irradiance in this treatment may explain the persistence of elevated chl *a* levels. PAR is often



285 negatively correlated with chl *a* content as higher chl *a* can help maintain elevated photosynthetic rates under  
reduced PAR (e.g. McWilliam and Naylor, 1967; Zhang et al., 2014). Bartsch et al. (2016) showed that the  
genus *Alaria* was more abundant than *Laminaria* and *Saccharina* between 10 and 15 m depth. Despite a  
decrease in irradiance caused by glacial and terrestrial runoff, *A. esculenta* is the only species that extended its  
maximum depth (from 15 to 18 m between 1994/96 to 2014; Bartsch et al., 2016). This shift could be explained  
290 by an effective short-term acclimation to low PAR, giving this species a competitive advantage at greater  
depth. Our findings shed light on the adaptive responses of *A. esculenta* to low light, and seemingly tolerance  
to low salinity and warming, suggesting that this species will most likely be able to withstand future coastal  
environmental conditions in the Arctic.

The chl *a* content of *L. digitata* and *S. latissima* was also not affected by the treatments. This is in agreement  
295 with the study of Diehl and Bischoff (2021) where temperature (up to 10°C), combined with low salinity (down  
to 25) did not affect the content of chl *a* of *S. latissima*. However, their growth rate in low light conditions  
remained similar to the other treatments. Other physiological processes such as photosynthetic efficiency, or  
resource allocation, might have been altered to maintain growth rates similar to the control.

#### 300 4.2 C:N ratio

The C:N ratio of *S. latissima* was significantly lower in the T2 treatment compared to  $t_0$ . The decrease in C:N  
ratio seems driven by an increase in nitrogen uptake. Benthic marine macroalgae and seagrasses from  
temperate and tropical regions have a mean C:N ratio of 22 (Atkinson and Smith, 1983). In northern Norway,  
Liesner et al. (2020) reported a C:N ratio of 21 for *L. digitata* which is consistent with our measurements for  
305 this species as well as for *A. esculenta*, all treatments and sampling times combined. However, *S. latissima*  
exhibited higher ratios with a mean of  $29.7 \pm 5.5$  ( $t_0$  and  $t_{\text{final}}$  of the control, T1 and T3 combined), which would  
suggest nitrogen limitation. While algae in the T2 treatment showed a higher nitrogen content, which is an  
essential nutrient playing a central role in photosynthesis and protein biosynthesis, the growth rate remained  
similar to the other treatments. Gordillo et al. (2002) showed higher nitrogen uptake at lower salinity (50% vs.  
310 100% seawater) in *Fucus serratus* that was explained by increased N metabolism. Thus, the higher nitrogen  
content found here in the low saline T2 treatment (salinity down to 28) could have resulted from increased N  
metabolism. Indeed, the increase in nitrogen concentration in the macroalgae can induce an increase in the  
activity of the nitrate reductase (Korb and Gerard, 2000). This enzyme catalyzes the first step in the reduction  
of nitrate to organic forms and protein synthesis. In fact, nitrate concentration in water was higher in T2 ( $1.68$   
315  $\pm 0.8 \mu\text{M/L}$ ) treatment than the control ( $0.87 \pm 0.9 \mu\text{M/L}$ , data not shown) during the duration of the  
experiment. Arctic coastal waters are known to be nitrate-limited (Santos-Garcia et al., 2022). The influx of  
fresh and potentially more nitrate-rich waters may have induced an increase in the N metabolism of *S. latissima*  
which was nitrogen limited. Higher nutrient input from land through coastal erosion and permafrost thawing  
may benefit this species in various processes such as photosynthesis, biosynthesis, immunity and/or molecule  
320 transport (Campbell, 1988; Meyer et al., 2005).



#### 4.3 Growth rate

We also hypothesized that warming may enhance the growth rate of kelp. None of the growth rates of the three study species were affected by the different treatments over the total duration of the experiment. In contrast, 325 previous studies observed an increase of the growth rate of *S. latissima* when exposed to warmer conditions (8-10°C vs. 0-4°C under replete irradiance; Iñiguez et al., 2016; Olischläger et al., 2017; Li et al., 2020; Diehl and Bischoff, 2021). This discrepancy with our results can be explained by the duration of the experiment (7 to 18 days in previous studies vs 6 weeks here), the study period, and the irradiance. Our study was performed at the end of the peak growth (mid-May to July) and after, while other studies were performed in early July or 330 used sporophytes raised from gametophyte cultures. The growth rate of *A. esculenta* significantly decreased over time in the control, indicating the gradual end of the growth peak, with many of the kelp starting to senesce (Fig. A1-A). For *S. latissima*, no significant differences were found over time in the C indicating that the experiment started after the growth peak (Fig. A1-B; Berge et al., 2020). In the T3 treatment only, growth was stimulated only during the first four weeks of the experiment, suggesting that warming may have prolonged 335 the growth rate of *S. latissima* after the end of the peak growth period. Further studies may focus on this aspect. The T2 treatment did not induce a growth stimulation suggesting a negative effect of salinity and/or low irradiance.

#### 4.4 Gene expression

340 Both *H. nigripes* and *S. latissima* exhibited different gene expressions in the control compared to the treatments. The fact that treatments are not clustered separately from each other but are grouped together against the control suggests that the common factor among them, which is the increase in temperature, might be the key influencing factor.

Interestingly, and as we hypothesized, the response to these treatments differed between the two species. 345 The analysis of DEGs shows that the low salinity and irradiance treatment (T2) had a higher impact on the number of genes regulated in *H. nigripes* while warming alone (T3) had a higher impact on genes regulation on *S. latissima*. Since no phenotypic response was observed for *S. latissima* in T3, this suggests that the observed down-regulation might be an acclimation mechanism enabling the organism to maintain its main processes. Other parameters could be measured to validate this hypothesis (lipid content, photosynthesis 350 rates, accessory pigment concentrations, etc). Li et al., (2020) found a regulation of genes involved to reduce the osmotic pressure under low-salinity stress in *S. latissima* (salinity of 20 vs. 30). We did not observe such results with this species nor with *H. nigripes*, most likely because the reduction in salinity was much smaller in our experiment (up to -5 here vs -10 in Li et al., 2020). However, for both species, T2 induced a down-regulation of photorespiratory genes. This is consistent with previous observations in *S. latissima* (Monteiro et al., 2019). Under stressful conditions like hyposalinity, kelp may prioritize acclimatization and survival strategies over photosynthesis. Photosynthesis was however not measured 355 during the experiment to validate this hypothesis.



Finally, we noticed a down-regulation, rather than the expected up-regulation, of heat-shock proteins (HSP), despite their typical induction under abiotic stress (Sørensen et al., 2003). The regulation of HSP  
360 in response to salinity variations occurs to a lesser degree compared to its response to temperature changes (Monteiro et al., 2019). Considering that these species originate from lower latitudes, their current exposure to the low temperatures in the Arctic might induce stress, while future warmer waters may reduce it.

#### 4.5 Future prospects of *Alaria esculenta*, *Saccharina latissima*, *Laminaria digitata*, and *Hedophyllum nigripes* 365 in the Arctic

Our findings support the hypothesis that *A. esculenta* is more likely to be resilient to future changes in irradiance than other kelp species. In particular, our results reveal its competitive advantage at depth, through its high content in chl *a*. No discernible positive impact of its higher chlorophyll *a* content was observed on  
370 its growth rate in low light conditions. This impact may be more evident earlier in the season, during the peak growth. *A. esculenta* seems resilient to increasing glacier and river runoff, becoming more dominant in low-light environments such as greater depths (Bartsch et al., 2016). The dominance of a single kelp species in specific regions may carry ecological consequences, as reduced diversity threatens ecosystem resilience.

For *L. digitata*, our results demonstrate neither negative nor positive effects of warming, low salinity, and low irradiance. Franke et al. (2021) also found no effect of a 5°C warming on the growth rate of this species  
375 (control: 5°C, warming: 10°C). However, in our study confusion with *H. nigripes* at  $t_0$  has split the data, making the analysis less robust. Indeed, the individuals could only be identified at the end of the experiment, after cutting the stipe. This led to the removal of 16 individuals from the analysis. The slight decrease in the content of chl *a* over time, as observed for the other two species in the study, could not be confirmed statistically. Bartsch et al. (2016) found that *L. digitata* was the only species that experienced a significant increase in  
380 biomass between 1994/1996 and 2014 on the entire transect they studied (from 0 to 15 m depth). Current and future conditions in the short term seem optimal for this species. Germination of *L. digitata* is enhanced at 9°C compared to 5°C and 15°C (Zacher et al., 2016, 2019) and its growth rate is higher at 15°C compared to 5°C and 10°C (Franke et al., 2021). Although warming alone may be beneficial to this species, its combined effects with other environmental factors might be detrimental once a certain threshold is reached. Muller et al., (2008)  
385 found no difference in the germination rate between 7°C and 12°C, but showed that germination under UV of type A and B decreased down to less than 30% at 12°C compared to almost 80% at 7°C.

*S. latissima* is widely studied throughout the northern hemisphere. In the Arctic specifically, several studies indicate that future conditions may favor the expansion of this species. This is supported by findings of enhanced germination with temperatures up to 12°C (Muller et al., 2008) and mitigation of the negative effects  
390 of UV radiation at high temperatures (12°C; Heinrich et al., 2015). Our results reveal that *S. latissima* may benefit from increasing N input from coastal erosion and permafrost thawing that could enhance immunity, photosynthesis, biosynthesis and/or molecule transport, although this was not measured in this study. *S. latissima* exhibits a high degree of polymorphism, acclimatation, and genetic diversity across populations



(Bartsch et al., 2008; Guzinski et al., 2016). For example, its growth shows a high phenotypic plasticity that  
395 appears to be constrained within specific seasonal patterns (Spurkland and Iken, 2011). In the Canadian Arctic,  
Goldsmith et al., (2021) found that suitable habitat of this species may gain 64,000 km<sup>2</sup> by 2050, most of this  
new area being in the northernmost reaches, where temperature is rising and sea ice is receding. Bartsch et al.  
(2016) found a 30-time increase in its biomass between 1994/1996 in 2014 at 2.5 m depth at Hansneset  
(Kongsfjorden, Svalbard, Norway). *S. latissima* will most likely benefit from future conditions although the  
400 capacity and time of dispersal, as well as competition with other species, predation, and extreme events must  
be considered for population projections.

So far, *A. esculenta*, *L. digitata*, and *S. latissima* have adapted successfully to the shifting Arctic environment  
and our results suggest that they might thrive in the conditions expected for 2100. In the short term, these  
species may well continue to spread in this region. Regarding *H. nigripes*, Franke et al. (2021) suggested a  
405 true Arctic affinity with a sporophyte growth optima of 10°C. By 2100, this species might continue to thrive  
in the Arctic, as evidenced by our gene expression analysis, which suggests efficient acclimatization with less  
stress under future scenarios.

Kelp species will, however, face more competition, grazing, and extreme events such as high sedimentation  
rate, ice-scouring, and marine heatwaves (Hu et al., 2020). Around Tromsø (Norway), the massive spread of  
410 sea urchins may have caused the ecosystem to collapse into a bare new state (Sivertsen et al., 1997). Moreover,  
with warming, the frequency and intensity of marine heatwaves will increase which could have important  
consequences on marine species of Arctic flora and fauna. These potential effects of climate change should be  
taken into account to better assess the future of Arctic kelp communities. It therefore appears essential to  
continue to study these communities in order to predict and anticipate future changes and impacts on fisheries,  
415 local and indigenous people, and on a global scale.

### Acknowledgment

We are grateful to the staff of the Alfred Wegener Institute (AWI), Institut polaire français Paul Emile Victor  
(IPEV), and Kings bay for field assistance. We thank Cátia Monteiro for her advice on RNA extraction and  
Erwan Corre for his expertise and guidance to process transcriptomic data. Thanks are also due to Inka Bartsch,  
420 Kai Bischof, and Simon Jungblut for their input, which improved the design and interpretation of this study,  
and Nathalie Leblond for her help with the CHN analysis. This study was conducted in the frame of the project  
FACE-IT (The Future of Arctic Coastal Ecosystems – Identifying Transitions in Fjord Systems and Adjacent  
Coastal Areas). FACE-IT has received funding from the European Union's Horizon 2020 research and  
innovation programme under grant agreement No 869154. We also acknowledge the support of IPEV (project  
425 ARCTOS 1248) and the Prince Albert II of Monaco Foundation (project ORCA n°3051).

### Competing interest

At least one of the (co-)authors is a member of the editorial board of Biogeosciences.



### Author contributions

AL, CM, SC, PU, SA, RS, JPG, and FG were involved in the fieldwork. AL, CM, SC, JPG, and FG designed  
430 the study. SC, PU, and FG designed the system. The experiment was conducted by AL, CM, SC, SA, RS, JPG,  
and FG. AL and CM performed measurements of the chl *a* content. AL performed the C:N ratio measurement  
and the RNA extractions. MM processed transcriptomic data. AL analyzed the data and wrote the first draft of  
the manuscript, which was then finalized by all co-authors.

### 435 References

- Aguilera, J., Bischof, K., Karsten, U., Hanelt, D., Wiencke, C., 2002. Seasonal variation in ecophysiological patterns in macroalgae from an Arctic fjord. II. Pigment accumulation and biochemical defence systems against high light stress. *Marine Biology* 140, 1087–1095. <https://doi.org/10.1007/s00227-002-0792-y>
- Ahmed, R., Prowse, T., Dibike, Y., Bonsal, B., O’Neil, H., 2020. Recent trends in freshwater influx to the  
440 Arctic Ocean from four major Arctic-draining rivers. *Water* 12, 1189.
- Atkinson, M.J., Smith, S.V., 1983. C:N:P ratios of benthic marine plants. *Limnology and Oceanography* 28, 568–574. <https://doi.org/10.4319/lo.1983.28.3.0568>
- Bartsch, I., Paar, M., Fredriksen, S., Schwanitz, M., Daniel, C., Hop, H., Wiencke, C., 2016. Changes in kelp forest biomass and depth distribution in Kongsfjorden, Svalbard, between 1996–1998 and 2012–2014 reflect  
445 Arctic warming. *Polar Biology* 39, 2021–2036.
- Bartsch, I., Wiencke, C., Bischof, K., Buchholz, C.M., Buck, B.H., Eggert, A., Feuerpfeil, P., Hanelt, D., Jacobsen, S., Karez, R., Karsten, U., Molis, M., Roleda, M.Y., Schubert, H., Schumann, R., Valentin, K., Weinberger, F., Wiese, J., 2008. The genus *Laminaria* sensu lato : recent insights and developments. *European Journal of Phycology* 43, 1–86. <https://doi.org/10.1080/09670260701711376>
- 450 Bates, D., Mächler, M., Bolker, B., Walker, S., 2015. Fitting linear mixed-effects models using lme4. *Journal of Statistical Software* 67. <https://doi.org/10.18637/jss.v067.i01>
- Bauer, S., Grossmann, S., Vingron, M., Robinson, P.N., 2008. Ontologizer 2.0—a multifunctional tool for GO term enrichment analysis and data exploration. *Bioinformatics* 24, 1650–1651.
- Berge, J., Johnsen, G., Cohen, J., 2020. Polar night marine ecology. *Advances in Polar Ecology* 4.
- 455 Bischof, K., Hanelt, D., Wiencke, C., 1999. Acclimation of maximal quantum yield of photosynthesis in the brown alga *Alaria esculenta* under high light and UV radiation. *Plant Biology* 1, 435–444. <https://doi.org/10.1111/j.1438-8677.1999.tb00726.x>
- Bolger, A.M., Lohse, M., Usadel, B., 2014. Trimmomatic: a flexible trimmer for Illumina sequence data. *Bioinformatics* 30, 2114–2120.
- 460 Bray, N.L., Pimentel, H., Melsted, P., Pachter, L., 2016. Near-optimal probabilistic RNA-seq quantification. *Nature biotechnology* 34, 525–527.
- Bushmanova, E., Antipov, D., Lapidus, A., Prjibelski, A.D., 2019. rnaSPAdes: a de novo transcriptome assembler and its application to RNA-Seq data. *GigaScience* 8, giz100.



- Campbell, W.H., 1988. Nitrate reductase and its role in nitrate assimilation in plants. *Physiologia Plantarum* 465 74, 214–219. <https://doi.org/10.1111/j.1399-3054.1988.tb04965.x>
- Dankworth, M., Heinrich, S., Fredriksen, S., Bartsch, I., 2020. DNA barcoding and mucilage ducts in the stipe reveal the presence of *Hedophyllum nigripes* (Laminariales, Phaeophyceae) in Kongsfjorden (Spitsbergen). *Journal of Phycology* 56, 1245–1254. <https://doi.org/10.1111/jpy.13012>
- Diehl, N., Bischof, K., 2021. Coping with a changing Arctic: mechanisms of acclimation in the brown seaweed 470 *Saccharina latissima* from Spitsbergen. *Marine Ecology Progress Series* 657, 43–57. <https://doi.org/10.3354/meps13532>
- Eggert, A., 2012. Seaweed Responses to Temperature, in: Wiencke, C., Bischof, K. (Eds.), *Seaweed biology: novel insights into ecophysiology, Ecology and Utilization*, Ecological Studies. Springer, Berlin, Heidelberg, pp. 47–66. [https://doi.org/10.1007/978-3-642-28451-9\\_3](https://doi.org/10.1007/978-3-642-28451-9_3)
- 475 Filbee-Dexter, K., Wernberg, T., Fredriksen, S., Norderhaug, K.M., Pedersen, M.F., 2019. Arctic kelp forests: diversity, resilience and future. *Global and Planetary Change* 172, 1–14. <https://doi.org/10.1016/j.gloplacha.2018.09.005>
- Finn, R.D., Clements, J., Eddy, S.R., 2011. HMMER web server: interactive sequence similarity searching. *Nucleic Acids Research* 39, W29–W37. <https://doi.org/10.1093/nar/gkr367>
- 480 Franke, K., Liesner, D., Heesch, S., Bartsch, I., 2021. Looks can be deceiving: contrasting temperature characteristics of two morphologically similar kelp species co-occurring in the Arctic. *Botanica Marina* 64, 163–175. <https://doi.org/10.1515/bot-2021-0014>
- Gene Ontology Consortium, 2015. Gene ontology consortium: going forward. *Nucleic acids research* 43, D1049–D1056.
- 485 Goldsmit, J., Schlegel, R.W., Filbee-Dexter, K., MacGregor, K.A., Johnson, L.E., Mundy, C.J., Savoie, A.M., McKindsey, C.W., Howland, K.L., Archambault, P., 2021. Kelp in the eastern Canadian Arctic: current and future predictions of habitat suitability and cover. *Frontiers in Marine Science* 18, 742209. <https://doi.org/10.3389/fmars.2021.742209>
- Gordillo, F., Dring, M., Savidge, G., 2002. Nitrate and phosphate uptake characteristics of three species of 490 brown algae cultured at low salinity. *Marine Ecology Progress Series* 234, 111–118. <https://doi.org/10.3354/meps234111>
- Grabherr, M.G., Haas, B.J., Yassour, M., Levin, J.Z., Thompson, D.A., Amit, I., Adiconis, X., Fan, L., Raychowdhury, R., Zeng, Q., 2011. Full-length transcriptome assembly from RNA-Seq data without a reference genome. *Nature biotechnology* 29, 644–652.
- 495 Guzinski, J., Mauger, S., Cock, J.M., Valero, M., 2016. Characterization of newly developed expressed sequence tag-derived microsatellite markers revealed low genetic diversity within and low connectivity between European *Saccharina latissima* populations. *Journal of Applied Phycology* 28, 3057–3070. <https://doi.org/10.1007/s10811-016-0806-7>
- Haas, B., Papanicolaou, A., 2015. *TransDecoder* 5.5. 0.





- 500 Heinrich, S., Frickenhaus, S., Glöckner, G., Valentin, K., 2012. A comprehensive cDNA library of light- and temperature-stressed *Saccharina latissima* (Phaeophyceae). *European Journal of Phycology* 47, 83–94. <https://doi.org/10.1080/09670262.2012.660639>
- Heinrich, S., Valentin, K., Frickenhaus, S., Wiencke, C., 2015. Temperature and light interactively modulate gene expression in *Saccharina latissima* (Phaeophyceae). *Journal of Phycology* 51, 93–108.  
505 <https://doi.org/10.1111/jpy.12255>
- Hop, H., Wiencke, C., Vögele, B., Kovaltchouk, N.A., 2012. Species composition, zonation, and biomass of marine benthic macroalgae in Kongsfjorden, Svalbard. *Botanica Marina* 55, 399–414. <https://doi.org/10.1515/bot-2012-0097>
- Hu, S., Zhang, L., Qian, S., 2020. Marine heatwaves in the Arctic region: variation in different ice covers.  
510 *Geophysical Research Letters* 47. <https://doi.org/10.1029/2020GL089329>
- Huerta-Cepas, J., Forslund, K., Coelho, L.P., Szklarczyk, D., Jensen, L.J., Von Mering, C., Bork, P., 2017. Fast genome-wide functional annotation through orthology assignment by eggNOG-Mapper. *Molecular Biology and Evolution* 34, 2115–2122. <https://doi.org/10.1093/molbev/msx148>
- Huerta-Cepas, J., Szklarczyk, D., Heller, D., Hernández-Plaza, A., Forslund, S.K., Cook, H., Mende, D.R.,  
515 Letunic, I., Rattei, T., Jensen, L.J., von Mering, C., Bork, P., 2019. eggNOG 5.0: a hierarchical, functionally and phylogenetically annotated orthology resource based on 5090 organisms and 2502 viruses. *Nucleic Acids Research* 47, D309–D314. <https://doi.org/10.1093/nar/gky1085>
- Iñiguez, C., Carmona, R., Lorenzo, M.R., Niell, F.X., Wiencke, C., Gordillo, F.J.L., 2016. Increased temperature, rather than elevated CO<sub>2</sub>, modulates the carbon assimilation of the Arctic kelps *Saccharina*  
520 *latissima* and *Laminaria solidungula*. *Marine Biology* 163, 248. <https://doi.org/10.1007/s00227-016-3024-6>
- Karsten, U., 2012. Seaweed Acclimation to Salinity and Desiccation Stress, in: Wiencke, C., Bischof, K. (Eds.), *Seaweed biology: novel insights into ecophysiology, ecology and utilization, ecological studies*. Springer, Berlin, Heidelberg, pp. 87–107. [https://doi.org/10.1007/978-3-642-28451-9\\_5](https://doi.org/10.1007/978-3-642-28451-9_5)
- Karsten, U., 2007. Research note: salinity tolerance of Arctic kelps from Spitsbergen. *Phycological Research*  
525 55, 257–262. <https://doi.org/10.1111/j.1440-1835.2007.00468.x>
- Korb, R.E., Gerard, V.A., 2000. Nitrogen assimilation characteristics of polar seaweeds from differing nutrient environments. *Marine Ecology Progress Series* 198, 83–92.
- Krause-Jensen, D., Archambault, P., Assis, J., Bartsch, I., Bischof, K., Filbee-Dexter, K., Dunton, K.H., Maximova, O., Ragnarsdóttir, S.B., Sejr, M.K., Simakova, U., Spiridonov, V., Wegeberg, S., Winding,  
530 M.H.S., Duarte, C.M., 2020. Imprint of climate change on pan-Arctic marine vegetation. *Frontiers in Marine Science* 7, 617324. <https://doi.org/10.3389/fmars.2020.617324>
- Krause-Jensen, D., Duarte, C.M., 2016. Substantial role of macroalgae in marine carbon sequestration. *Nature Geoscience* 9, 737–742. <https://doi.org/10.1038/ngeo2790>
- Krause-Jensen, D., Marbà, N., Olesen, B., Sejr, M.K., Christensen, P.B., Rodrigues, J., Renaud, P.E., Balsby,  
535 T.J.S., Rysgaard, S., 2012. Seasonal sea ice cover as principal driver of spatial and temporal variation in depth extension and annual production of kelp in Greenland. *Global Change Biology* 18, 2981–2994. <https://doi.org/10.1111/j.1365-2486.2012.02765.x>





- Kwiatkowski, L., Torres, O., Bopp, L., Aumont, O., Chamberlain, M., Christian, J.R., Dunne, J.P., Gehlen, M., Ilyina, T., John, J.G., Lenton, A., Li, H., Lovenduski, N.S., Orr, J.C., Palmieri, J., Santana-Falcón, Y.,  
540 Schwinger, J., Séférian, R., Stock, C.A., Tagliabue, A., Takano, Y., Tjiputra, J., Toyama, K., Tsujino, H.,  
Watanabe, M., Yamamoto, A., Yool, A., Ziehn, T., 2020. Twenty-first century ocean warming, acidification,  
deoxygenation, and upper-ocean nutrient and primary production decline from CMIP6 model projections.  
*Biogeosciences* 17, 3439–3470. <https://doi.org/10.5194/bg-17-3439-2020>
- Lebrun, A., Comeau, S., Gazeau, F., Gattuso, J.-P., 2022. Impact of climate change on Arctic macroalgal  
545 communities. *Global and Planetary Change* 103980.
- Letunic, I., Khedkar, S., Bork, P., 2021. SMART: recent updates, new developments and status in 2020.  
*Nucleic Acids Research* 49, D458–D460. <https://doi.org/10.1093/nar/gkaa937>
- Li, H., Monteiro, C., Heinrich, S., Bartsch, I., Valentin, K., Harms, L., Glöckner, G., Corre, E., Bischof, K.,  
2020. Responses of the kelp *Saccharina latissima* (Phaeophyceae) to the warming Arctic: from physiology to  
550 transcriptomics. *Physiologia Plantarum* 168, 5–26. <https://doi.org/10.1111/ppl.13009>
- Li, W., Godzik, A., 2006. Cd-hit: a fast program for clustering and comparing large sets of protein or nucleotide  
sequences. *Bioinformatics* 22, 1658–1659. <https://doi.org/10.1093/bioinformatics/btl158>
- Liesner, D., Fouqueau, L., Valero, M., Roleda, M.Y., Pearson, G.A., Bischof, K., Valentin, K., Bartsch, I.,  
2020. Heat stress responses and population genetics of the kelp *Laminaria digitata* (Phaeophyceae) across  
555 latitudes reveal differentiation among North Atlantic populations. *Ecology and Evolution* 10, 9144–9177.  
<https://doi.org/10.1002/ece3.6569>
- Lorenzen, C.J., 1967. Determination of chlorophyll and pheopigments: spectrophotometric equations.  
*Limnology and Oceanography* 12, 343–346. <https://doi.org/10.4319/lo.1967.12.2.0343>
- Love, M.I., Huber, W., Anders, S., 2014. Moderated estimation of fold change and dispersion for RNA-seq  
560 data with DESeq2. *Genome Biology* 15, 550. <https://doi.org/10.1186/s13059-014-0550-8>
- McWilliam, J.R., Naylor, A.W., 1967. Temperature and plant adaptation. I. Interaction of temperature and  
light in the synthesis of chlorophyll in corn. *Plant Physiology* 42, 1711–1715.  
<https://doi.org/10.1104/pp.42.12.1711>
- Meyer, C., Lea, U.S., Provan, F., Kaiser, W.M., Lillo, C., 2005. Is nitrate reductase a major player in the plant  
565 NO (nitric oxide) game? *Photosynthesis Research* 83, 181–189. <https://doi.org/10.1007/s11120-004-3548-3>
- Millard, S.P., 2013. *EnvStats: An R Package for Environmental Statistics*. Springer, New York. ISBN 978-1-  
4614-8455-4, <https://www.springer.com>.
- Miller, C.A., Urrutti, P., Gattuso, J.-P., Comeau, S., Lebrun, A., Alliouane, S., Schlegel, R.W., Gazeau, F.,  
n.d. Technical note: an autonomous flow through salinity and temperature perturbation mesocosm system for  
570 multi-stressor experiments (preprint). *Biodiversity and Ecosystem Function: Marine*.  
<https://doi.org/10.5194/egusphere-2023-768>
- Mistry, J., Chuguransky, S., Williams, L., Qureshi, M., Salazar, G.A., Sonnhammer, E.L.L., Tosatto, S.C.E.,  
Paladin, L., Raj, S., Richardson, L.J., Finn, R.D., Bateman, A., 2021. Pfam: The protein families database in  
2021. *Nucleic Acids Research* 49, D412–D419. <https://doi.org/10.1093/nar/gkaa913>



- 575 Monteiro, C.M.M., Li, H., Bischof, K., Bartsch, I., Valentin, K.U., Corre, E., Collén, J., Harms, L., Glöckner, G., Heinrich, S., 2019. Is geographical variation driving the transcriptomic responses to multiple stressors in the kelp *Saccharina latissima*? *BMC Plant Biol* 19, 513. <https://doi.org/10.1186/s12870-019-2124-0>
- Müller, R., Laepple, T., Bartsch, I., Wiencke, C., 2009. Impact of oceanic warming on the distribution of seaweeds in polar and cold-temperate waters. *Botanica Marina* 52, 617–638.  
580 <https://doi.org/10.1515/BOT.2009.080>
- Müller, R., Wiencke, C., Bischof, K., 2008. Interactive effects of UV radiation and temperature on microstages of Laminariales (Phaeophyceae) from the Arctic and North Sea. *Climate Research* 37, 203–213. <https://doi.org/10.3354/cr00762>
- Muth, A.F., Bonsell, C., Dunton, K.H., 2021. Inherent tolerance of extreme seasonal variability in light and  
585 salinity in an Arctic endemic kelp (*Laminaria solidungula*). *Journal of Phycology* 57, 1554–1562. <https://doi.org/10.1111/jpy.13187>
- Olischläger, M., Iñiguez, C., Koch, K., Wiencke, C., Gordillo, F.J.L., 2017. Increased pCO<sub>2</sub> and temperature reveal ecotypic differences in growth and photosynthetic performance of temperate and Arctic populations of *Saccharina latissima*. *Planta* 245, 119–136. <https://doi.org/10.1007/s00425-016-2594-3>
- 590 Parke, M., 1948. Studies on British Laminariaceae. I. Growth in *Laminaria Saccharina* (L.) Lamour. *Journal of the Marine Biological Association of the United Kingdom* 27, 651–709. <https://doi.org/10.1017/S0025315400056071>
- Peterson, B.J., Holmes, R.M., McClelland, J.W., Vörösmarty, C.J., Lammers, R.B., Shiklomanov, A.I., Shiklomanov, I.A., Rahmstorf, S., 2002. Increasing River Discharge to the Arctic Ocean. *Science* 298, 2171–  
595 2173. <https://doi.org/10.1126/science.1077445>
- R Core Team, 2023. R: A language and environment for statistical computing. R Foundation for Statistical Computing, Vienna, Austria. URL <https://www.R-project.org/>
- Renaud, P.E., Wallhead, P., Kotta, J., Włodarska-Kowalczyk, M., Bellerby, R.G., Rätsep, M., Slagstad, D., Kukliński, P., 2019. Arctic sensitivity? Suitable habitat for benthic taxa is surprisingly robust to climate  
600 change. *Frontiers in Marine Science* 6, 538.
- Richter-Menge, J., Overland, J.E., Mathis, J.T., Osborne, E., 2017. Arctic Report Card: Arctic shows no sign of returning to reliably frozen region of recent past decades.
- Roleda, M., Wiencke, C., Hanelt, D., 2005. Response of Arctic kelp zoospores to ultraviolet and photosynthetically active radiation in relation to growth depth. 8th International Phycological Congress, 13–  
605 19 August 2005, Durban, South Africa.
- Santos-Garcia, M., Ganeshram, R.S., Tuerena, R.E., Debyser, M.C.F., Husum, K., Assmy, P., Hop, H., 2022. Nitrate isotope investigations reveal future impacts of climate change on nitrogen inputs and cycling in Arctic fjords: Kongsfjorden and Rijpfjorden (Svalbard). *Biogeosciences* 19, 5973–6002. <https://doi.org/10.5194/bg-19-5973-2022>
- 610 Scherrer, K.J.N., Kortsch, S., Varpe, Ø., Weyhenmeyer, G.A., Gulliksen, B., Primicerio, R., 2019. Mechanistic model identifies increasing light availability due to sea ice reductions as cause for increasing macroalgae cover in the Arctic: light causes arctic macroalgal increase. *Limnology and Oceanography* 64, 330–341. <https://doi.org/10.1002/lno.11043>



Shiklomanov, I.A., Shiklomanov, A.I., 2003. Climatic change and the dynamics of river runoff into the Arctic  
615 Ocean. *Water Resources* 30, 593–601.

Simão, F.A., Waterhouse, R.M., Ioannidis, P., Kriventseva, E.V., Zdobnov, E.M., 2015. BUSCO: assessing  
genome assembly and annotation completeness with single-copy orthologs. *Bioinformatics* 31, 3210–3212.  
<https://doi.org/10.1093/bioinformatics/btv351>

Sivertsen, K., 1997. Geographic and environmental factors affecting the distribution of kelp beds and barren  
620 grounds and changes in biota associated with kelp reduction at sites along the Norwegian coast. *Canadian  
Journal of Fisheries and Aquatic Sciences* 54, 2872–2887. <https://doi.org/10.1139/f97-186>

Sørensen, J.G., Kristensen, T.N., Loeschcke, V., 2003. The evolutionary and ecological role of heat shock  
proteins: Heat shock proteins. *Ecology Letters* 6, 1025–1037. <https://doi.org/10.1046/j.1461-0248.2003.00528.x>

625 Springer, K., Lütz, C., Lütz-Meindl, U., Wendt, A., Bischof, K., 2017. Hyposaline conditions affect UV  
susceptibility in the Arctic kelp *Alaria esculenta* (Phaeophyceae). *Phycologia* 56, 675–685.  
<https://doi.org/10.2216/16-122.1>

Spurkland, T., Iken, K., 2011. Salinity and irradiance effects on growth and maximum photosynthetic quantum  
yield in subarctic *Saccharina latissima* (Laminariales, Laminariaceae). *Botanica Marina* 54.  
630 <https://doi.org/10.1515/bot.2011.042>

Stroeve, J.C., Markus, T., Boisvert, L., Miller, J., Barrett, A., 2014. Changes in Arctic melt season and  
implications for sea ice loss. *Geophysical Research Letters* 41, 1216–1225.  
<https://doi.org/10.1002/2013GL058951>

Supek, F., Bošnjak, M., Škunca, N., Šmuc, T., 2011. REVIGO Summarizes and Visualizes Long Lists of Gene  
635 Ontology Terms. *PLoS ONE* 6, e21800. <https://doi.org/10.1371/journal.pone.0021800>

Vihtakari M (2023). ggOceanMaps: plot data on oceanographic maps using 'ggplot2'. R package version 2.0.4,  
<https://mikkovihtakari.github.io/ggOceanMaps/>

Wiencke, C., Bartsch, I., Bischoff, B., Peters, A.F., Breeman, A.M., 1994. Temperature requirements and  
biogeography of Antarctic, Arctic and Amphiequatorial Seaweeds. *Botanica Marina* 37.  
640 <https://doi.org/10.1515/botm.1994.37.3.247>

Zacher, K., Bernard, M., Bartsch, I., Wiencke, C., 2016. Survival of early life history stages of Arctic kelps  
(Kongsfjorden, Svalbard) under multifactorial global change scenarios. *Polar Biology* 39, 2009–2020.  
<https://doi.org/10.1007/s00300-016-1906-1>

Zacher, K., Bernard, M., Daniel Moreno, A., Bartsch, I., 2019. Temperature mediates the outcome of species  
645 interactions in early life-history stages of two sympatric kelp species. *Marine Biology* 166, 161.  
<https://doi.org/10.1007/s00227-019-3600-7>

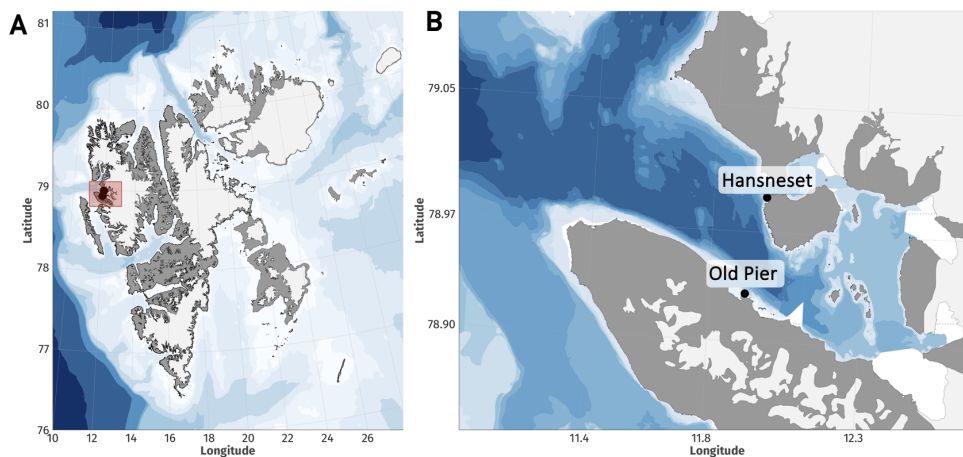
Zhang, D.-W., Yuan, S., Xu, F., Zhu, F., Yuan, M., Ye, H.-X., Guo, H.-Q., Lv, X., Yin, Y., Lin, H.-H., 2016.  
Light intensity affects chlorophyll synthesis during greening process by metabolite signal from mitochondrial  
alternative oxidase in *A. rabiopsis*: Signalling by AOX regulates greening process. *Plant, Cell & Environment*  
650 39, 12–25. <https://doi.org/10.1111/pce.12438>

**Table 1: Temperature, salinity, and photosynthetically active radiation during the experiment. T1 and T2 treatments represent future coastline exposed to runoff conditions, whereas T3 treatment represents future conditions on shores**



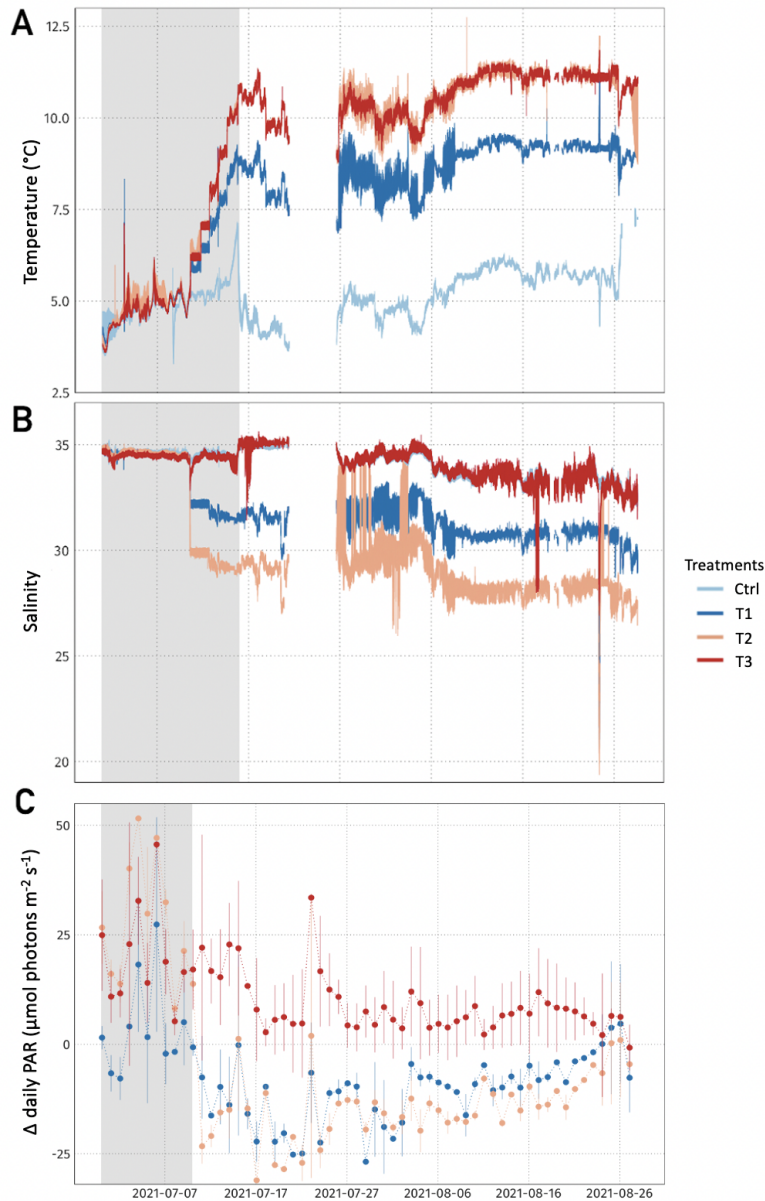
655 not exposed to runoff. The quartiles and medians were calculated based on data acquired from 2021-07-10 for Photosynthetically Active Radiation (PAR) and 2021-07-16 for temperature and salinity (once the targeted treatments were reached) until the end of the experiment.

Treatment	Scenario	Temperature (°C)				Salinity				daily PAR ( $\mu\text{mol photons m}^{-2} \text{s}^{-1}$ )			
		$\Delta$	1st quartile	Median	3rd quartile	$\Delta$	1st quartile	Median	3rd quartile	$\Delta$	1st quartile	Median	3rd quartile
Ctrl	control	<i>in situ</i>	4.8	5.3	5.8	<i>in situ</i>	33.4	33.8	34.3	<i>in situ</i>	35.1	47.8	59.5
T1	SSP2-4.5 - coastline	+ 3.3°C	8.4	8.9	9.2	- 2.5	30.8	31.0	31.8	- 20 %	27.8	36.1	43.9
T2	SSP5-8.5 - coastline	+ 5.3°C	10.3	10.8	11.2	- 5	28.2	28.5	29.5	- 30 %	23.8	31.4	40.7
T3	SSP5-8.5 - offshore	+ 5.3°C	10.3	10.8	11.2	<i>in situ</i>	33.4	33.9	34.5	<i>in situ</i>	40.3	54.8	69.9



660

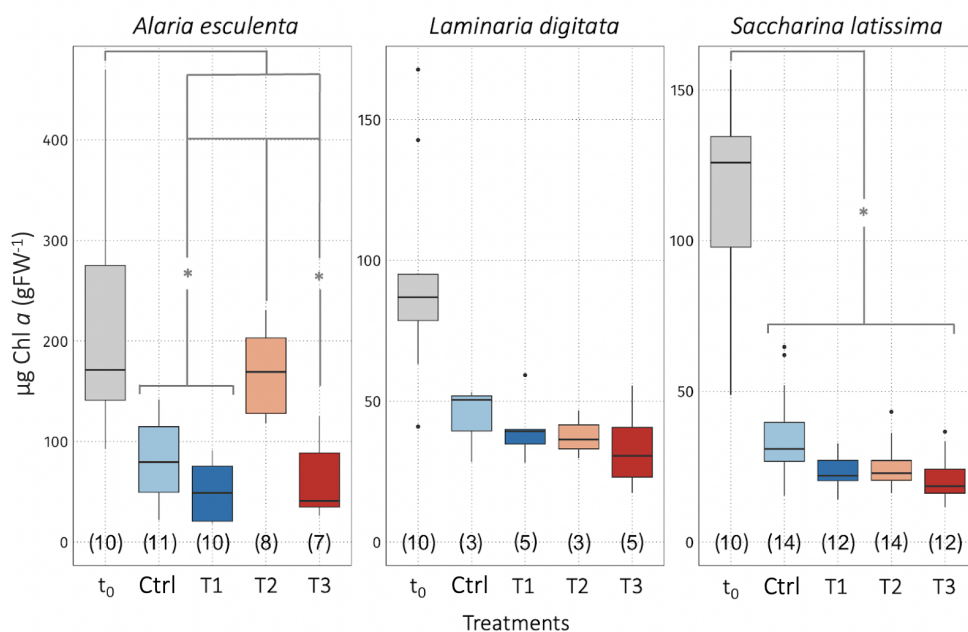
Figure 1: The study was carried out in Svalbard (A) on kelp sampled in Kongsfjorden (B) in Hansneset and the Old Pier. Maps were created using the R package ggOceanMaps (Vihtakari, 2023).



665

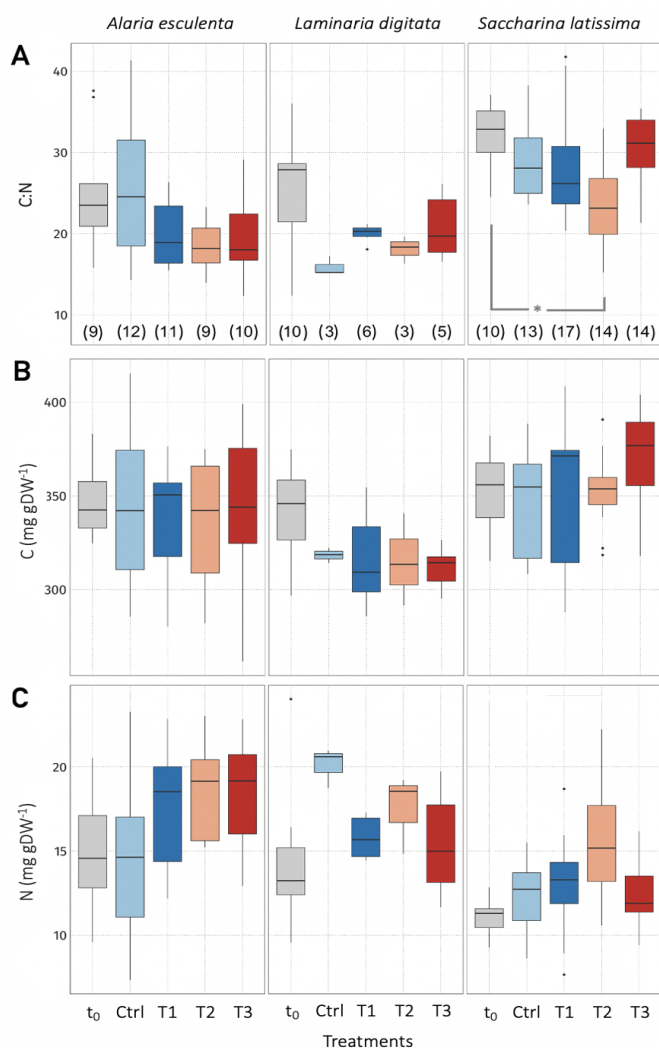
Figure 2: A) Temperature, B) salinity, and C)  $\Delta$  Daily Photosynthetically Active Radiation (PAR) between the control and the treatments. Temperature, salinity, and PAR were measured every minute. PAR values were integrated over 10-minute intervals and averaged over the day. The gray-shaded region corresponds to the beginning of the experiment, before the treatment conditions of temperature, salinity and irradiance were reached. A few days of temperature and salinity data were lost (from 2021-07-21 to 2021-07-26).

670



675 **Figure 3: Chlorophyll *a* (chl *a*) content of *Alaria esculenta*, *Laminaria digitata*, and *Saccharina latissima* exposed to the four treatments, expressed per unit of fresh weight (gFW). t<sub>0</sub> values correspond to the chl *a* content at the start of the experiment, while Ctrl, T1, T2, and T3 correspond to the final chl *a* content of organisms maintained in the respective treatments for six weeks. The horizontal lines in each boxplot represent the median. The whiskers extend to the furthest data points within 1.5 times the interquartile range (the top and bottom of the box). Statistically significant differences are shown with an asterisk (p < 0.05). The number in parentheses below each boxplot corresponds to the sample size.**

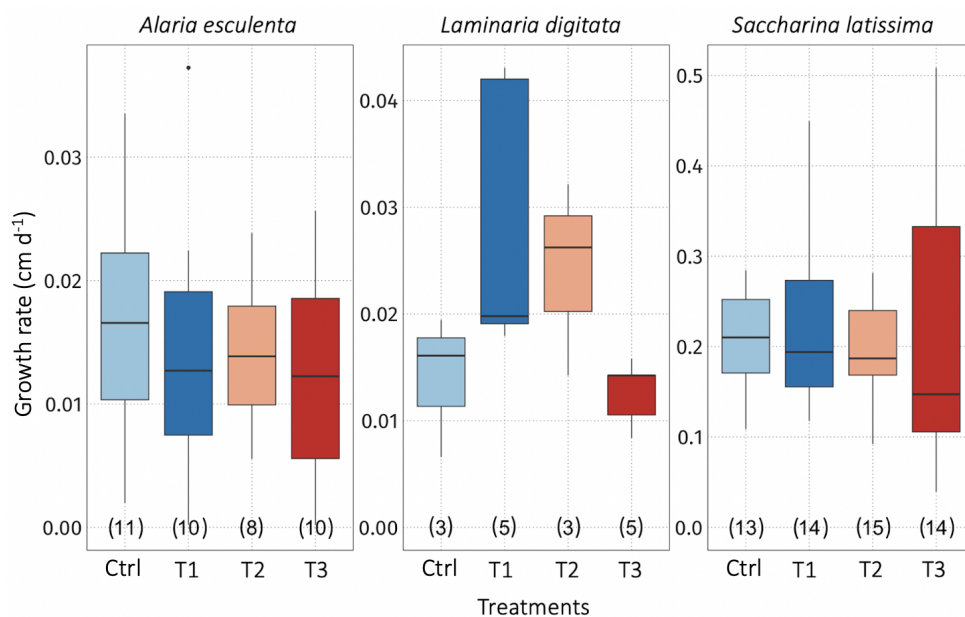




680

**Figure 4:** A) Carbon:nitrogen (C:N), B) carbon contents, and C) nitrogen contents of *Alaria esculenta*, *Laminaria digitata*, and *Saccharina latissima* exposed to the four treatments, expressed per unit of dry weight (gDW). t<sub>0</sub> values correspond to samples taken at the start of the experiment, while Ctrl, T1, T2, and T3 correspond to the final values from organisms maintained in the respective treatments for six weeks. The horizontal lines in each boxplot represent the median. The whiskers extend to the furthest data points within 1.5 times the interquartile range (the top and bottom of the box). Statistically significant differences are shown with an asterisk ( $p < 0.05$ ). The number in parentheses below each boxplot in (A) corresponds to the sample size, respectively the same in (B) and (C).

685



690

**Figure 5:** Growth rate of *Alaria esculenta*, *Laminaria digitata*, and *Saccharina latissima* exposed to the four treatments during six weeks. The horizontal lines in each boxplot represent the median. The horizontal lines in each boxplot represent the median. The whiskers extend to the furthest data points within 1.5 times the interquartile range (the top and bottom of the box). The number in parentheses below each boxplot corresponds to the sample size.

695



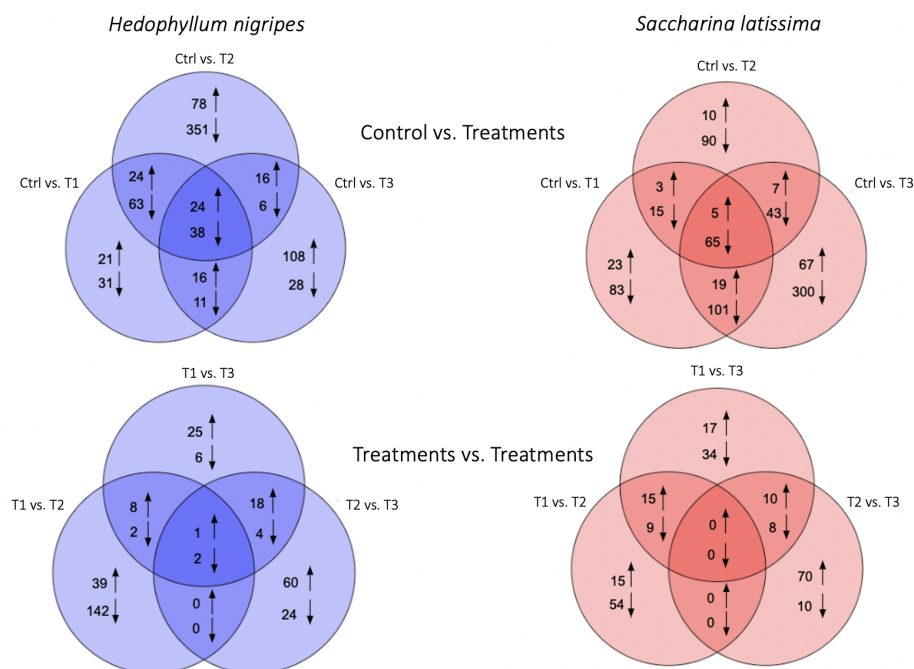
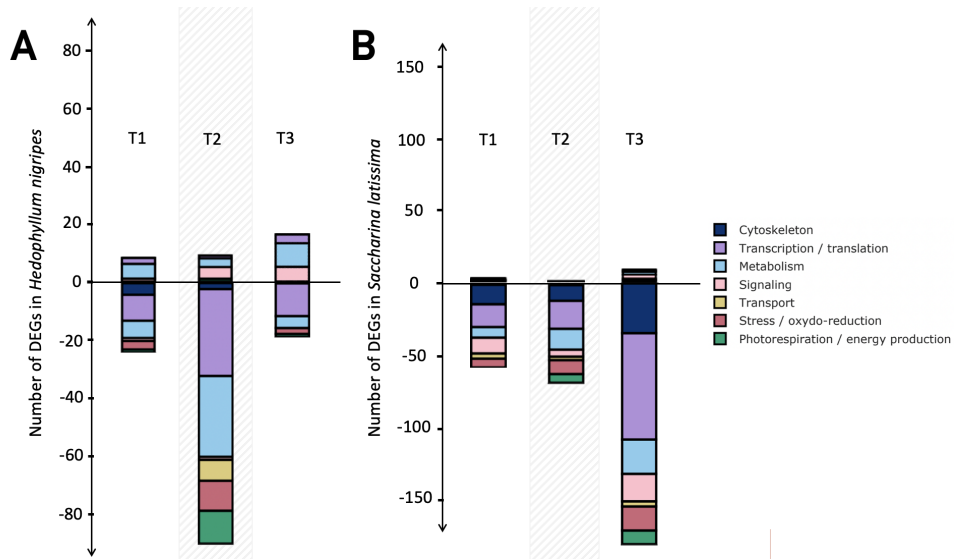


**Figure 6: Venn diagrams of differentially up-regulated (↑) and down-regulated (↓) genes of *Saccharina latissima* and *Hedophyllum nigripes* between the control and the treatments (T1, T2, and T3) and between treatments.**

700

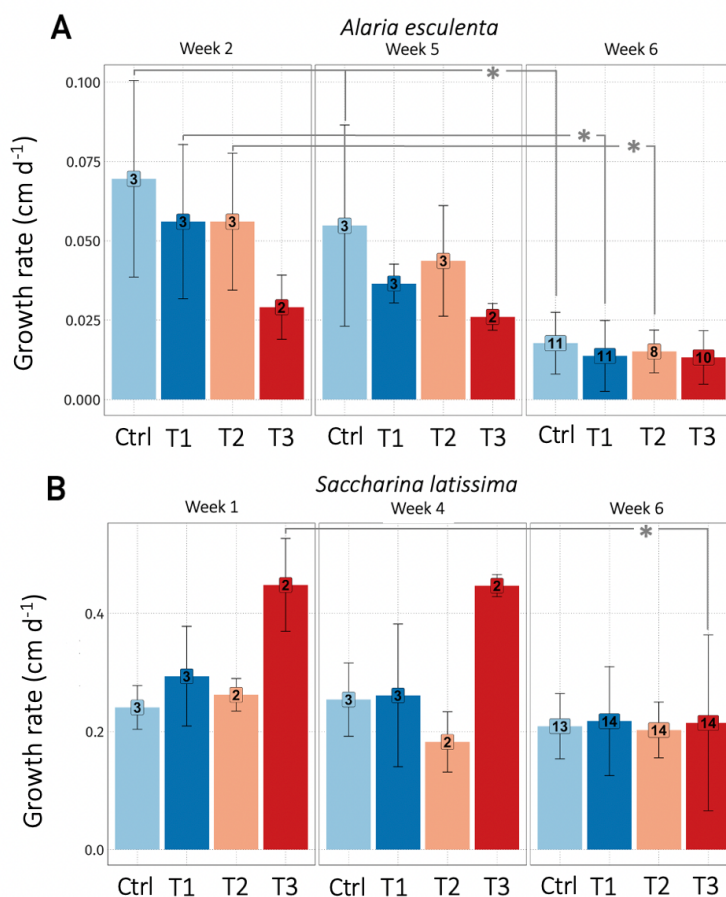


705 **Figure 7:** Number of classified differentially expressed genes (degs) in **A) Hedophyllum nigripes** and **B) Saccharina latissima** in response to T1, T2, and T3. The upper part of the graph displays up-regulated degs and the lower part down-regulated degs. Genes were classified with their Pfam and eggnog annotations (see 2.7).



Appendices

Appendices A



710 Figure A1: Growth rate calculated at different intervals during the experiment within treatments for A) *Alaria*  
715 *esculenta* (Week 0 to 2, 2 to 5, and 5 to 6), and B) *Saccharina latissima* (Weeks 0 to 1, 1 to 4, and 4 to 6). The number on  
each barplot corresponds to the sample size. *Laminaria digitata* was not represented due to its low sample size in week  
3. Values from  $t_0$  to week 6 are represented in Figure 5. A generalized linear mixed model (GLMM) with a Gaussian  
distribution was used to test for the effects of the species, treatment, time, and mesocosm replica. No significant  
differences were found between mesocosm replicas. Statistically significant differences are shown with an asterisk ( $p <$   
0.05).

720

725



Appendice B

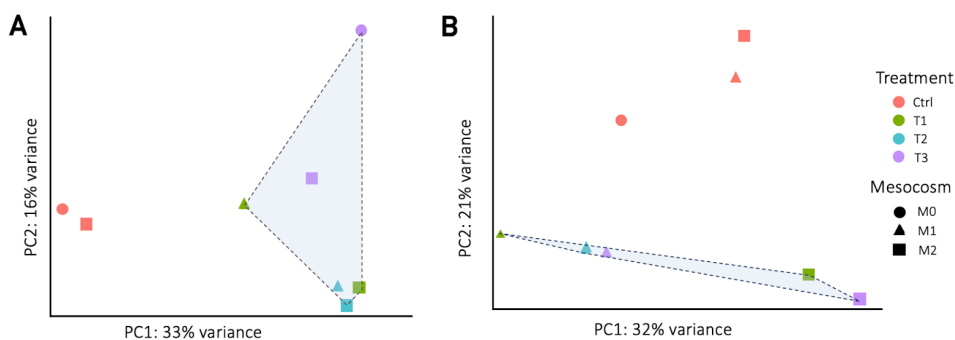


**Fig. B1: Principal Component Analysis of the expressed genes in the control and treatments of A) *Hedophyllum nigripes* and B) *Saccharina latissima*. Treatments T1, T2, and T3 are grouped in the blue geometrical figures.**

730 Appendice C

**Table C1: Tools and parameters used for transcriptomic data processing.**

Tool	Version	Arguments and parameters
FastQC	0.11.7	-o \$outputDirectory
Trimmomatic	0.39	PE -threads 10 -phred33 -trimlog LEADING:3 TRAILING:3 SLIDINGWINDOW:4:15 MINLEN:36 TruSeq3-PE.fa:2:30:10
Trinity	2.14.0	--seqType fq --max_memory 128G --samples_file \$sampleFiles --CPU 32 --output \$outputDirectory --full_cleanup
CD-HIT	4.8.1	-i \$transcriptome -o \$output -c 0.95 -n 8
rnaSPAdes	3.14.1	--pe1-1 \$seq1 --pe1-2 \$seq2 [...] --pe4-1 \$seq7 --pe4-2 \$seq8 -o \$output_directory
BUSCO	5.4.3	--in \$transcriptome --out \$output -c 24 -l /\$pathDB/eukaryota_odb10 --config \$config --mode transcriptome
Kallisto	0.46.0	quant -i \$index -o \$outputDirectory -b 100 -t 16 \$seq1 \$seq2
DESeq2	1.34.0	Counts recovery via txImport (files=DesignFile, type='Kallisto', tx2gene=tx2geneFile) Contrasts depends on biological questions with alpha=0.05
TransDecoder	5.5.0	LongOrfs : \$transcriptome Predict : \$transcriptome
HMMER	3.3	--domtblout \$output -E 1e-10 --cpu 16 \$pfamDB \$transdecoderLongestOrf
eggNOG-mapper	2.1.10	-i \$transdecoderLongestOrf -o \$eggnogAnnot
Ontologizer	2.1	-a \$associationFile -g \$goDB -s \$studySamples -p \$populationFile -c Parent-Child-Union -o \$outputDirectory -d 0.05 -r 1000



735 Appendice D

**Table D1: Analysis of deviance (Type II Wald chi-square tests) in a linear mixed model with a hierarchical structure to predict the chlorophyll *a* contents.**

	Chisq	Df	Pr(>Chisq)
species	91.310	2	<2.2e-16 ***
treatment	98.991	4	<2.2e-16 ***
species:treatment	39.729	8	3.599e-06 ***

740

**Table D2: Pairwise comparisons of the chlorophyll *a* values calculated by the method of Tukey on a linear mixed model with a hierarchical structure (fixed factors: treatment and species, random factor: mesocosm). The p-values in bold (< 0.05) support the hypothesis that there is a significant difference in the pair. AE: *Alaria esculenta*, LD: *Laminaria digitata*, SL: *Saccharina latissima***

Species	Treatment vs.	Species	Treatment	estimate	SE	df	t.ratio	p.value
AE	t0 -	LD	t0	124.75	18.6	117.0	6.708	<b>&lt;.0001</b>
AE	t0 -	SL	t0	104.37	18.6	117.0	5.612	<b>&lt;.0001</b>
AE	t0 -	AE	Ctrl	136.06	19.0	22.9	7.146	<b>&lt;.0001</b>
AE	t0 -	AE	T1	167.96	19.3	25.6	8.706	<b>&lt;.0001</b>
AE	t0 -	AE	T2	48.68	20.4	30.6	2.388	0.5405
AE	t0 -	AE	T3	155.52	21.2	33.5	7.325	<b>&lt;.0001</b>
LD	t0 -	SL	t0	-20.38	18.6	117.0	-1.096	0.9988
LD	t0 -	LD	Ctrl	49.65	27.8	69.5	1.783	0.8967
LD	t0 -	LD	T1	54.29	24.0	38.6	2.260	0.6231
LD	t0 -	LD	T2	56.08	27.8	69.5	2.014	0.7829
LD	t0 -	LD	T3	60.95	23.5	43.6	2.588	0.4048
SL	t0 -	LD	Ctrl	70.03	27.8	69.5	2.515	0.4437
SL	t0 -	SL	Ctrl	79.06	18.0	20.0	4.396	<b>0.0158</b>
SL	t0 -	SL	T1	90.64	18.5	22.2	4.887	<b>0.0044</b>
SL	t0 -	SL	T2	89.20	18.0	19.9	4.953	<b>0.0049</b>
SL	t0 -	SL	T3	93.45	18.6	21.9	5.019	<b>0.0034</b>
AE	Ctrl -	LD	Ctrl	38.33	27.2	117.8	1.409	0.9850
AE	Ctrl -	SL	Ctrl	47.36	17.0	118.9	2.779	0.2727
AE	Ctrl -	AE	T1	31.89	18.4	118.7	1.733	0.9184
AE	Ctrl -	AE	T2	-87.38	19.4	117.9	-4.497	<b>0.0015</b>



AE	Ctrl	-	AE	T3	19.46	20.3	118.6	0.958	0.9997
LD	Ctrl	-	SL	Ctrl	9.04	26.5	117.2	0.341	1.0000
LD	Ctrl	-	LD	T1	4.64	30.9	119.0	0.150	1.0000
LD	Ctrl	-	LD	T2	6.43	34.0	117.0	0.190	1.0000
LD	Ctrl	-	LD	T3	11.30	30.5	118.0	0.370	1.0000
SL	Ctrl	-	LD	T1	-4.40	22.6	115.7	-0.194	1.0000
SL	Ctrl	-	SL	T1	11.58	16.5	118.4	0.702	1.0000
SL	Ctrl	-	SL	T2	10.14	15.7	117.4	0.644	1.0000
SL	Ctrl	-	SL	T3	14.39	16.4	117.3	0.878	0.9999
AE	T1	-	LD	T1	11.08	23.6	117.3	0.469	1.0000
AE	T1	-	SL	T1	27.05	17.9	118.0	1.511	0.9722
AE	T1	-	AE	T2	-119.27	19.7	117.2	-6.040	<b>&lt;.0001</b>
AE	T1	-	AE	T3	-12.43	20.7	118.6	-0.600	1.0000
LD	T1	-	SL	T1	15.98	22.6	119.0	0.707	1.0000
LD	T1	-	LD	T2	1.79	30.9	119.0	0.058	1.0000
LD	T1	-	LD	T3	6.66	26.4	118.0	0.252	1.0000
SL	T1	-	SL	T2	-1.44	16.6	118.8	-0.087	1.0000
SL	T1	-	SL	T3	2.81	17.2	118.9	0.163	1.0000
AE	T2	-	LD	T2	132.14	28.2	117.1	4.691	<b>0.0007</b>
AE	T2	-	SL	T2	144.88	18.4	117.1	7.856	<b>&lt;.0001</b>
AE	T2	-	AE	T3	106.84	21.7	118.4	4.920	<b>0.0003</b>
LD	T2	-	SL	T2	12.74	26.5	117.3	0.481	1.0000
LD	T2	-	LD	T3	4.87	30.5	118.0	0.159	1.0000
SL	T2	-	SL	T3	4.25	16.4	117.6	0.259	1.0000
AE	T3	-	LD	T3	30.17	24.5	118.1	1.231	0.9959
AE	T3	-	SL	T3	42.29	20.2	119.0	2.091	0.7381
LD	T3	-	SL	T3	12.12	22.6	119.0	0.537	1.0000

745

750



755 Appendice E

**Table E1: C:N ratios (A), carbon contents (B), and nitrogen contents as a function of the treatment were investigated with an analysis of deviance (Type II Wald chi-square tests) in a linear mixed model with a hierarchical structure.**

A		Chisq	Df	Pr(>Chisq)
	species	61.003	2	5.667e-14 ***
	treatment	29.275	4	6.872e-06 ***
	species:treatment	11.285	8	0.1861

B		Chisq	Df	Pr(>Chisq)
	species	23.8694	2	6.559e-06 ***
	treatment	3.8547	4	0.4260
	species:treatment	6.0497	8	0.6417

C		Chisq	Df	Pr(>Chisq)
	species	51.647	2	6.096e-12 ***
	treatment	25.979	4	3.196e-05 ***
	species:treatment	14.373	8	0.07254

760 **Table E2: Pairwise comparisons of A) the C:N ratios, B) the carbon contents, C) the nitrogen contents calculated by the method of Tukey on a linear mixed model with a hierarchical structure (fixed factors: treatment and species, random factor: mesocosm). The p-values in bold (< 0.05) indicates a significant difference in the pair. AE: *Alaria esculenta*, LD: *Laminaria digitata*, SL: *Saccharina latissima*.**

A	Species	Treatment	vs. Species	Treatment	estimate	SE	df	t.ratio	p.value	
	AE	t0	-	LD	t0	-0.1152	2.63	125.0	-0.044	1.0000
	AE	t0	-	SL	t0	-6.7996	2.56	125.0	-2.654	0.3458
	AE	t0	-	AE	Ctrl	-0.4640	2.47	41.0	-0.187	1.0000
	AE	t0	-	AE	T1	5.2689	2.51	45.0	2.100	0.7276
	AE	t0	-	AE	T2	6.7233	2.83	58.0	2.378	0.5403
	AE	t0	-	AE	T3	5.8060	2.56	47.8	2.264	0.6201



LD	t0	-	SL	t0	-6.6845	2.56	125.0	-2.609	0.3746
LD	t0	-	LD	Ctrl	9.4646	3.72	98.2	2.546	0.4190
LD	t0	-	LD	T1	5.3231	2.99	58.9	1.783	0.8955
LD	t0	-	LD	T2	7.2351	3.72	98.2	1.946	0.8236
LD	t0	-	LD	T3	4.4934	3.14	69.9	1.431	0.9814
SL	t0	-	SL	Ctrl	2.9358	2.36	36.1	1.246	0.9937
SL	t0	-	SL	T1	3.6898	2.22	31.4	1.659	0.9302
SL	t0	-	SL	T2	8.5439	2.32	34.5	3.686	<b>0.0453</b>
SL	t0	-	SL	T3	1.5997	2.36	35.2	0.677	1.0000
AE	Ctrl	-	LD	Ctrl	9.8134	3.61	125.6	2.718	0.3066
AE	Ctrl	-	SL	Ctrl	-3.3998	2.28	126.8	-1.490	0.9755
AE	Ctrl	-	AE	T1	5.7328	2.34	126.1	2.449	0.4841
AE	Ctrl	-	AE	T2	7.1873	2.67	126.2	2.694	0.3206
AE	Ctrl	-	AE	T3	6.2700	2.41	126.7	2.599	0.3810
LD	Ctrl	-	SL	Ctrl	-13.2133	3.58	125.5	-3.692	<b>0.0247</b>
LD	Ctrl	-	LD	T1	-4.1415	3.98	126.7	-1.041	0.9993
LD	Ctrl	-	LD	T2	-2.2295	4.55	125.0	-0.490	1.0000
LD	Ctrl	-	LD	T3	-4.9712	4.09	126.2	-1.214	0.9965
SL	Ctrl	-	SL	T1	0.7539	2.07	126.7	0.363	1.0000
SL	Ctrl	-	SL	T2	5.6081	2.17	126.8	2.581	0.3927
SL	Ctrl	-	SL	T3	-1.3361	2.21	126.6	-0.606	1.0000
AE	T1	-	LD	T1	-0.0609	2.90	126.3	-0.021	1.0000
AE	T1	-	SL	T1	-8.3787	2.16	125.5	-3.875	<b>0.0136</b>
AE	T1	-	AE	T2	1.4545	2.72	126.7	0.535	1.0000
AE	T1	-	AE	T3	0.5372	2.44	125.2	0.220	1.0000
LD	T1	-	SL	T1	-8.3178	2.69	126.9	-3.086	0.1367
LD	T1	-	LD	T2	1.9120	3.98	126.7	0.481	1.0000
LD	T1	-	LD	T3	-0.8297	3.38	125.1	-0.246	1.0000
SL	T1	-	SL	T2	4.8542	2.02	126.2	2.398	0.5214
SL	T1	-	SL	T3	-2.0900	2.08	127.0	-1.004	0.9995
AE	T2	-	LD	T2	0.3966	3.86	125.7	0.103	1.0000
AE	T2	-	SL	T2	-4.9791	2.61	126.9	-1.907	0.8453
AE	T2	-	AE	T3	-0.9173	2.78	126.8	-0.330	1.0000
LD	T2	-	SL	T2	-5.3757	3.55	125.4	-1.513	0.9721





LD	T2	-	LD	T3	-2.7417	4.09	126.2	-0.670	1.0000
SL	T2	-	SL	T3	-6.9442	2.15	125.7	-3.223	0.0967
AE	T3	-	LD	T3	-1.4278	3.09	126.9	-0.462	1.0000
AE	T3	-	SL	T3	-11.0059	2.36	126.1	-4.669	<b>0.0007</b>
LD	T3	-	SL	T3	-9.5782	3.02	125.3	-3.173	0.1101

**B Species Treatment vs. Species Treatment estimate SE df t.ratio p.value**

					estimate	SE	df	t.ratio	p.value
AE	t0	-	LD	t0	5.634	14.1	125.0	0.400	1.0000
AE	t0	-	SL	t0	-6.839	13.7	125.0	-0.498	1.0000
AE	t0	-	AE	Ctrl	3.002	13.3	41.0	0.226	1.0000
AE	t0	-	AE	T1	8.934	13.4	45.0	0.664	1.0000
AE	t0	-	AE	T2	10.408	15.2	58.0	0.687	1.0000
AE	t0	-	AE	T3	1.157	13.7	47.8	0.084	1.0000
LD	t0	-	SL	t0	-12.473	13.7	125.0	-0.908	0.9999
LD	t0	-	LD	Ctrl	21.981	19.9	98.2	1.103	0.9987
LD	t0	-	SL	Ctrl	-7.587	13.0	39.6	-0.583	1.0000
LD	t0	-	LD	T1	24.351	16.0	58.9	1.521	0.9679
LD	t0	-	LD	T2	25.098	19.9	98.2	1.259	0.9947
LD	t0	-	LD	T3	28.694	16.8	69.9	1.705	0.9244
SL	t0	-	SL	Ctrl	4.886	12.6	36.1	0.387	1.0000
SL	t0	-	SL	T1	0.176	11.9	31.4	0.015	1.0000
SL	t0	-	SL	T2	-0.691	12.4	34.5	-0.056	1.0000
SL	t0	-	SL	T3	-18.336	12.7	35.2	-1.447	0.9761
AE	Ctrl	-	LD	Ctrl	24.612	19.4	125.6	1.272	0.9944
AE	Ctrl	-	SL	Ctrl	-4.956	12.2	126.8	-0.405	1.0000
AE	Ctrl	-	AE	T1	5.932	12.5	126.1	0.473	1.0000
AE	Ctrl	-	AE	T2	7.406	14.3	126.2	0.518	1.0000
AE	Ctrl	-	LD	T2	27.730	19.4	125.6	1.433	0.9827
AE	Ctrl	-	AE	T3	-1.845	12.9	126.7	-0.143	1.0000
LD	Ctrl	-	SL	Ctrl	-29.568	19.2	125.5	-1.541	0.9674
LD	Ctrl	-	LD	T1	2.370	21.3	126.7	0.111	1.0000
LD	Ctrl	-	SL	T1	-34.278	18.7	125.0	-1.831	0.8810
LD	Ctrl	-	LD	T2	3.117	24.4	125.0	0.128	1.0000
LD	Ctrl	-	LD	T3	6.713	22.0	126.2	0.306	1.0000



SL	Ctrl	-	SL	T1	-4.710	11.1	126.7	-0.424	1.0000
SL	Ctrl	-	SL	T2	-5.577	11.6	126.8	-0.479	1.0000
SL	Ctrl	-	SL	T3	-23.222	11.8	126.6	-1.963	0.8153
AE	T1	-	LD	T1	21.051	15.5	126.3	1.355	0.9896
AE	T1	-	SL	T1	-15.598	11.6	125.5	-1.345	0.9903
AE	T1	-	AE	T2	1.474	14.6	126.7	0.101	1.0000
AE	T1	-	AE	T3	-7.777	13.1	125.2	-0.595	1.0000
LD	T1	-	SL	T1	-36.648	14.4	126.9	-2.537	0.4227
LD	T1	-	LD	T2	0.747	21.3	126.7	0.035	1.0000
LD	T1	-	LD	T3	4.343	18.1	125.1	0.240	1.0000
SL	T1	-	LD	T2	37.396	18.7	125.0	1.997	0.7962
SL	T1	-	SL	T2	-0.867	10.9	126.2	-0.080	1.0000
SL	T1	-	SL	T3	-18.512	11.2	127.0	-1.658	0.9414
AE	T2	-	AE	T3	-9.251	14.9	126.8	-0.621	1.0000
LD	T2	-	SL	T2	-38.262	19.1	125.4	-2.008	0.7896
LD	T2	-	LD	T3	3.596	22.0	126.2	0.164	1.0000
SL	T2	-	SL	T3	-17.645	11.6	125.7	-1.528	0.9697
AE	T3	-	LD	T3	33.171	16.6	126.9	2.001	0.7940
AE	T3	-	SL	T3	-26.332	12.6	126.1	-2.084	0.7429
LD	T3	-	SL	T3	-59.503	16.2	125.3	-3.677	<b>0.0259</b>

C Species Treatment vs. Species Treatment estimate SE df t.ratio p.value

					estimate	SE	df	t.ratio	p.value
AE	t0	-	LD	t0	0.2529	1.44	125.0	0.176	1.0000
AE	t0	-	SL	t0	3.5217	1.40	125.0	2.508	0.4423
AE	t0	-	AE	Ctrl	0.0322	1.36	41.0	0.024	1.0000
AE	t0	-	AE	T1	-2.8539	1.37	45.0	-2.077	0.7425
AE	t0	-	AE	T2	-3.8535	1.55	58.0	-2.487	0.4650
AE	t0	-	AE	T3	-3.8036	1.41	47.8	-2.707	0.3318
LD	t0	-	SL	t0	3.2689	1.40	125.0	2.328	0.5718
LD	t0	-	LD	Ctrl	-5.7111	2.04	98.2	-2.804	0.2626
LD	t0	-	LD	T1	-1.4098	1.64	58.9	-0.862	0.9999
LD	t0	-	LD	T2	-3.1407	2.04	98.2	-1.542	0.9665
LD	t0	-	LD	T3	-1.0560	1.72	69.9	-0.614	1.0000
SL	t0	-	SL	Ctrl	-1.1248	1.29	36.1	-0.871	0.9999



SL	t0	-	SL	T1	-1.8877	1.22	31.4	-1.550	0.9576
SL	t0	-	SL	T2	-4.5131	1.27	34.5	-3.554	0.0622
SL	t0	-	SL	T3	-1.3004	1.30	35.2	-1.004	0.9993
AE	Ctrl	-	LD	Ctrl	-5.4905	1.98	125.6	-2.776	0.2740
AE	Ctrl	-	SL	Ctrl	2.3647	1.25	126.8	1.892	0.8529
AE	Ctrl	-	AE	T1	-2.8861	1.28	126.1	-2.251	0.6282
AE	Ctrl	-	AE	T2	-3.8856	1.46	126.2	-2.659	0.3426
AE	Ctrl	-	AE	T3	-3.8358	1.32	126.7	-2.902	0.2102
LD	Ctrl	-	SL	Ctrl	7.8552	1.96	125.5	4.006	<b>0.0087</b>
LD	Ctrl	-	LD	T1	4.3014	2.18	126.7	1.973	0.8098
LD	Ctrl	-	LD	T2	2.5704	2.49	125.0	1.030	0.9994
LD	Ctrl	-	LD	T3	4.6552	2.24	126.2	2.075	0.7485
SL	Ctrl	-	SL	T1	-0.7629	1.14	126.7	-0.671	1.0000
SL	Ctrl	-	SL	T2	-3.3883	1.19	126.8	-2.846	0.2368
SL	Ctrl	-	SL	T3	-0.1756	1.21	126.6	-0.145	1.0000
AE	T1	-	LD	T1	1.6970	1.59	126.3	1.069	0.9991
AE	T1	-	SL	T1	4.4880	1.18	125.5	3.788	<b>0.0181</b>
AE	T1	-	AE	T2	-0.9995	1.49	126.7	-0.670	1.0000
AE	T1	-	AE	T3	-0.9497	1.34	125.2	-0.711	1.0000
LD	T1	-	SL	T1	2.7910	1.48	126.9	1.890	0.8536
LD	T1	-	AE	T2	-2.6966	1.72	126.8	-1.568	0.9623
LD	T1	-	LD	T2	-1.7310	2.18	126.7	-0.794	1.0000
LD	T1	-	LD	T3	0.3538	1.85	125.1	0.191	1.0000
SL	T1	-	SL	T2	-2.6254	1.11	126.2	-2.367	0.5439
SL	T1	-	SL	T3	0.5873	1.14	127.0	0.515	1.0000
AE	T2	-	LD	T2	0.9656	2.12	125.7	0.456	1.0000
AE	T2	-	SL	T2	2.8621	1.43	126.9	2.001	0.7942
AE	T2	-	AE	T3	0.0498	1.52	126.8	0.033	1.0000
LD	T2	-	SL	T2	1.8965	1.95	125.4	0.974	0.9997
LD	T2	-	LD	T3	2.0848	2.24	126.2	0.929	0.9998
SL	T2	-	SL	T3	3.2127	1.18	125.7	2.721	0.3047
AE	T3	-	LD	T3	3.0005	1.69	126.9	1.771	0.9051
AE	T3	-	SL	T3	6.0250	1.29	126.1	4.665	<b>0.0007</b>
LD	T3	-	SL	T3	3.0244	1.65	125.3	1.829	0.8818



765

Appendice F

770 **Table F1: Analysis of deviance (Type II Wald chi-square tests) in a generalized linear mixed model to predict the growth rate.**

	Chisq	Df	Pr(>Chisq)
species	91.310	2	<2.2e-16 ***
treatment	98.991	4	<2.2e-16 ***
species:treatment	39.729	8	3.599e-06 ***

775 **Table F2: Pairwise comparisons of the growth rates calculated by the method of Tukey generalized linear mixed model. The p-values in bold (< 0.05) support the hypothesis that there is a significant difference in the pair. AE: *Alaria esculenta*, LD: *Laminaria digitata*, SL: *Saccharina latissima*.**

Species	Treatment vs.	Species	Treatment	estimate	SE	df	t.ratio	p.value
AE	Ctrl -	LD	Ctrl	-6.78e-03	0.0327	115	-0.207	1.0000
AE	Ctrl -	SL	Ctrl	-1.87e-01	0.0264	115	-7.090	<b>&lt;.0001</b>
AE	Ctrl -	AE	T1	4.08e-03	0.0275	115	0.148	1.0000
AE	Ctrl -	AE	T2	2.62e-03	0.0299	115	0.088	1.0000
AE	Ctrl -	AE	T3	4.49e-03	0.0282	115	0.159	1.0000
LD	Ctrl -	SL	Ctrl	-1.80e-01	0.0318	115	-5.672	<b>&lt;.0001</b>
LD	Ctrl -	LD	T1	-2.73e-03	0.0340	115	-0.080	1.0000
LD	Ctrl -	LD	T2	3.85e-03	0.0358	115	0.107	1.0000
LD	Ctrl -	LD	T3	9.32e-03	0.0340	115	0.275	1.0000
SL	Ctrl -	SL	T1	-1.54e-02	0.0248	115	-0.622	1.0000
SL	Ctrl -	SL	T2	4.00e-03	0.0244	115	0.164	1.0000
SL	Ctrl -	SL	T3	-9.63e-03	0.0248	115	-0.388	1.0000
AE	T1 -	LD	T1	-1.36e-02	0.0290	115	-0.469	1.0000
AE	T1 -	SL	T1	-2.07e-01	0.0260	115	-7.961	<b>&lt;.0001</b>
AE	T1 -	AE	T2	-1.45e-03	0.0299	115	-0.049	1.0000
AE	T1 -	AE	T3	4.14e-04	0.0282	115	0.015	1.0000
LD	T1 -	SL	T1	-1.93e-01	0.0275	115	-7.014	<b>&lt;.0001</b>
LD	T1 -	LD	T2	6.57e-03	0.0325	115	0.202	1.0000
LD	T1 -	SL	T2	-1.74e-01	0.0272	115	-6.392	<b>&lt;.0001</b>



LD	T1	-	LD	T3	1.20e-02	0.0304	115	0.397	1.0000
LD	T1	-	SL	T3	-1.87e-01	0.0275	115	-6.803	<b>&lt;.0001</b>
SL	T1	-	SL	T2	1.94e-02	0.0239	115	0.812	0.9996
SL	T1	-	SL	T3	5.81e-03	0.0244	115	0.239	1.0000
AE	T2	-	LD	T2	-5.56e-03	0.0333	115	-0.167	1.0000
AE	T2	-	SL	T2	-1.86e-01	0.0282	115	-6.586	<b>&lt;.0001</b>
AE	T2	-	AE	T3	1.87e-03	0.0306	115	0.061	1.0000
LD	T2	-	SL	T2	-1.80e-01	0.0295	115	-6.111	<b>&lt;.0001</b>
LD	T2	-	LD	T3	5.48e-03	0.0325	115	0.169	1.0000
SL	T2	-	SL	T3	-1.36e-02	0.0239	115	-0.569	1.0000
AE	T3	-	LD	T3	-1.95e-03	0.0296	115	-0.066	1.0000
AE	T3	-	SL	T3	-2.01e-01	0.0267	115	-7.545	<b>&lt;.0001</b>
LD	T3	-	SL	T3	-1.99e-01	0.0275	115	-7.241	<b>&lt;.0001</b>